DEVELOPMENT OF NOVEL POTENTIAL OF PLASMA POLYMERIZATION TECHNIQUES FOR SURFACE MODIFICATION

TOTA PIRDO KASIH

A dissertation submitted to
Graduate School of Engineering Gunma University
for The Degree of
Doctor of Engineering

February, 2007

DEVELOPMENT OF NOVEL POTENTIAL OF PLASMA POLYMERIZATION TECHNIQUES FOR SURFACE MODIFICATION

CONTENTS

1. Chapter I **1**

General Introduction

2. Chapter II **19**

Development and Characterization of a Novel Non-equilibrium Atmospheric Pressure Plasma Torch

3. Chapter III **38**

Poly(methyl methacrylate) Films Deposited via Non-equilibrium Atmospheric Pressure Plasma Polymerization with Using Argon as the Working Gas

4. Chapter IV **57**

Non-equilibrium Atmospheric Pressure Argon Plasma Torch For Deposition of Thin Silicon Oxide Film

5. Chapter V **82**

Surface Modification of Kenaf Fiber via Plasma-induced Graft Polymerization

6. Chapter VI **103**

Summary

List of Achievements **106**

Acknowledgement **108**

Referee in-Chief	**: Professor H. Kubota**
Referees	**: Professor M. Unno**
	Professor R. Katakai
	Professor S. Tobita
	Professor T. Komoto

ABSTRACT

Plasma polymerization technique includes plasma(-state) polymerization and plasma-induced graft polymerization and it is one of the most powerful method for surface modification of polymeric materials. Base on the unsolved problems that still exist on the usage of plasma polymerization in industrial application, the works described in this thesis are intended to explore the application of the plasma discharge either for deposition of thin solid films using a newly developed non-equilibrium atmospheric pressure plasma torch as well as for inducing graft polymerization on plant fibers under low pressure condition.

The major part of the thesis is directed toward the development of a novel non-equilibrium atmospheric pressure plasma torch with its name: CAPPLAT (Cold Atmosphere Pressure Plasma Torch) and exploring the use of it for depositing plasma polymerized films having organic and inorganic features. The torch consists of a 4 mm inner diameter metal pipe (inner electrode) surrounded by a silicone tube (dielectric) and a metal belt of 20 mm wide (outer electrode) is placed around the silicone tube at its end. The temperature of the generated plasma jet is as low as room temperature. When the rare gas was used to generate the discharge, electrical diagnostic exhibited the homogeneous glow type discharge. Optical emission spectroscopy confirmed the inclusion of air component to the plasma jet. By selecting the applied voltage and gas flow rate, a proper condition for sufficient plasma jet length could be adjusted.

Applications of the torch have been realized to deposit both of organic and inorganic thin films. The organic film of plasma polymerized methyl methacrylate

(PPMMA) obtained by using argon (Ar) plasma torch has been found to be chemically and spectroscopically similar to that of conventional PMMA. This could be happened when the rate of MMA-carrying Ar gas was high enough to change the filamentary character of Ar plasma to the glow-like one. For the deposition of thin film from hexamethyldisiloxne (HMDSO) monomer with the inorganic character, it was found that the plasma generated by using Ar as the working gas was more effective than helium (He) plasma in terms of both quality and deposition rate of film at the same applied power, frequency and gas composition. This could be realized by adjusting the oxygen feed through the HMDSO bubbler. Moreover, the appearance of the film could be improved when a small amount nitrogen (N_2) was admixed to the Ar as a feed gas. The Ar/N_2 mixed gas by the composition of 30/1 was found to result in homogeneous appearance of discharge and could deposit the SiO_2-like film with better quality at the similar growth rate to the deposition by pure Ar plasma.

Plasma-induced graft polymerization of methyl methacrylate (MMA) onto kenaf fiber was studied with using a low pressure non-equilibrium plasma. The graft polymerization onto plant fiber with high content of lignin was successfully achieved by introducing peroxides on the fiber through plasma treatment. Vinyl monomer was chosen in order to change the hydrophylic surface of kenaf onto hydrophobic one without sacrifying its potential bulk properties. The chemical structure and morphology of the grafted surface fiber have been characterized by FT-IR, XPS and SEM analyses. Those characterizations indicated that the kenaf fiber was partially coated by PMMA. Nevertheless, judging from the results of TG/DTG study, the graft polymerized kenaf fiber has higher thermal stability than untreated one.

CHAPTER I

GENERAL INTRODUCTION

1.1. Plasma and State of The Art

Plasma is physically defined as an ionized gas in a neutral state with an equal number of positively and negatively charged particles (quasi-neutral). It consists of free electrons, radicals, ions, UV-radiation, and various highly excited neutral and charged species independent of the gases used. The entire plasma is electrically neutral, but its behavior is complex because the particles motions are controlled by electric and magnetic fields. In 1879 Sir William Crookes firstly defined this state of ionized gas as `*the fourth state of matter*` after solid, liquid and gas. The term of `*plasma*` itself has been introduced by Irving Langmuir[1] when he studied the electrified gases in vacuum tubes in 1928. Gases usually become ionized only when heated to very high temperatures (>5000°C), so plasma is usually a very hot substance. However, if the degree of gas ionization is very weak, low temperature plasma can also be generated, which is usually realized by electrical discharge.[2] Well known examples of plasmas are the sun and other stars in the universe which have temperatures ranging from 5000 to 70000°K and consist entirely of plasma.[3] Lightning, an electric discharge in air, can be considered as a plasma as well. These are the examples of natural and human-uncontrolled plasma. Man-made controlled

plasmas can be generated usually by electric device and have been used in industry for many years for a number of diverse applications. Fluorescent lamps, neon tubes and gas lasers are the actualization of man-made plasma devices.

According to the gas temperature, plasma can be classified into two types: thermal or equilibrium plasma which is fully ionized (gas temperature, $T_g \approx$ electron temperature, T_e) and cold (low temperature) or non-equilibrium plasma with the gas only partially ionized ($T_g \ll T_e$). Thermal plasma implies that the temperature of all active species (electron, ion and neutral) is the same. In practical application, it is typically used where heat is required, such as for cutting, welding, spraying or evaporation of analyte material in analytical ICP.[4] Cold plasma on the other hand plays an essential role in many fields of plasma processing in which the heat is not desirable such as for etching and deposition. The temperature of neutral and positively charged species is low, while the electrons are relatively in much higher temperature because they are light and easily accelerated by the applied electromagnetic fields. As a result the generated plasma is in the state of non-equilibrium and the reaction may proceed at low temperature, possibly to as low as room temperature. Consequently, cold plasma is well suited for the treatment or surface modification of temperature-sensitive materials.

There are various ways to supply necessary energy for plasma generation such as laser beams, flames and adiabatic compression. However, application of electric field is by far the most common method for plasma ignition. Direct current (DC) discharges, pulsed DC discharges, radio frequency (RF) discharges (13.56 MHz) and

microwave discharges (2.45 GHz) are the plasmas categorization based on electric apparatus. These common standard frequencies were chosen in order not to make interfering with telecommunication.[5] In technical applications, low temperature plasmas may be produced by those types of electrical sources. The basic feature of a variety of electrical discharges is that they produce plasmas in which the majority of the electrical energy primarily goes into production of energetic electrons, instead of heating the entire gas stream.[6] These energetic electrons induce ionization, excitation and molecular fragmentation process of the background gas molecules to produce excited species, free radicals and ions as well as additional electrons, leading to a complex mixture of active species which environmentally `*chemically-rich*`. Due to its essential role, the electrons are therefore considered to be the `*primary agents*` in the plasma.

1.2. Low Temperature Plasma Parameters

Plasma is broadly characterized by the following basic parameters: plasma density, degree of ionization and electron energy distribution. Plasma density refers to the particle number densities of electrons, n_e, and is approximately equal to the density of the ions, n_i, by the assumption of plasma quasi-neutrality. One of the most important plasma types for technical application is `*glow discharge*`, and the mechanism of the gas discharge can be explained by the following idea. In between of two electrodes placed in a gas a few electrons are emitted due to the omnipresent cosmic radiation. When a sufficiently high potential difference is applied to the

electrodes, the electrons are accelerated by the electric field and promoting ionization and other activation processes through the collision reactions with the gas atoms. When the electric field strength is high enough and some requirements such as pressure, gas nature and reactor design are fulfilled, this leads to *electrical breakdown* of the gas, which results in a self-sustaining discharge. The most important collisions are the inelastic collisions, leading to excitation and ionization. The excitation collisions followed by light emission of de-excitation are responsible for the glow characteristic of the discharge, while the ionization collisions create new electrons and ions and lead to the increasing of ionization degree to about 10^{-6}-10^{-3}. The steady state of glow discharge is obtained when the charge loss due to gas phase or surface recombination is compensated by new ionizations. Due to the strongly influence of electrons to the plasma properties, it is important to characterize the plasma by its electron energy distribution function (EEDF). This parameter can be used to determine the electron temperature (T_e) which distincts a variety types of plasmas. The shape of the EEDF depends on the energy lost via electron collisions and the energy gained by the time-dependent electric field in the plasma. Maxwell and Druyvesteyn distribution are the better approximation of the electron energy distribution for the low pressure plasma where the temperature of electrons is considered much higher than that of the ions, and when it assumed that the only energy loses are by elastic collisions. Figure 1.1 shows their distribution function for different average electron energies. For low-pressure plasmas containing mainly inert gases the electrons distribution can be characterized by a Maxwellian EEDF, although

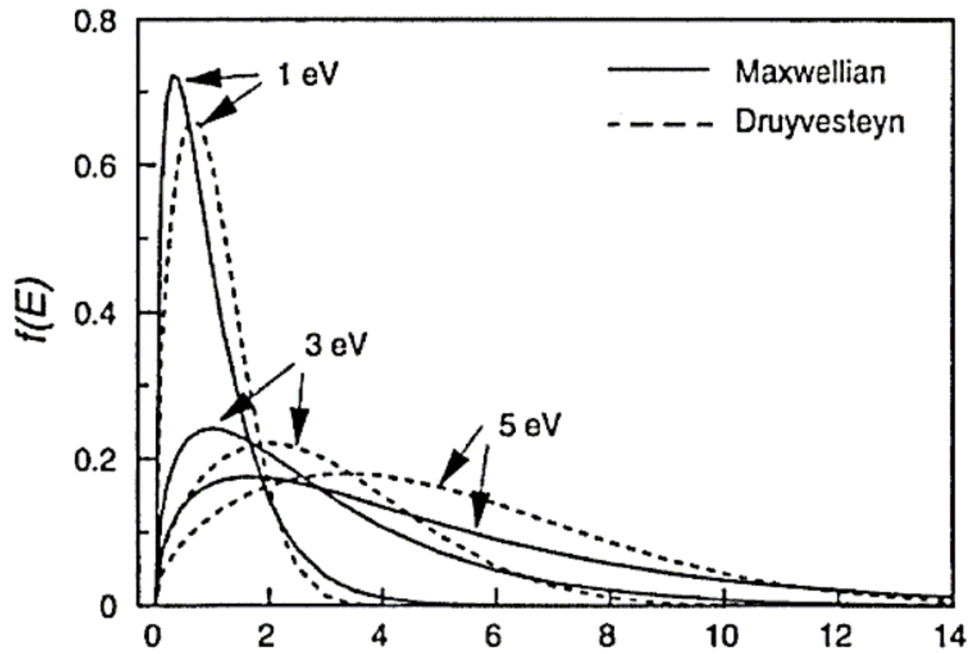

Figure 1.1 Electron energy distribution according to Maxwell and Druyvesteyn for three different average electron energies.[8]

the deviations have been reported.[7] However, most of discharges are not characterized by Maxwell distribution, particularly when using admixed gases or gaseous monomer. Both energy distributions show that the bulk of the electrons belong to the low-energy electrons (0.5–5 eV) while a small number of electrons have relatively high energies (5–14 eV). This high-energy tail region, however, plays an important role for dissociation and ionization reactions since those reactions have an energetic threshold and only happen if the energy of the participating electrons is higher.

Electrons determine the plasma characteristics as they are responsible for elastic and inelastic collisions. In elastic collisions the internal energy of the neutrals are unchanged, whereas the energy, momentum, and direction of the electrons undergo large changes. In inelastic collisions the energy that is transferred from the electron to the neutral species, causes many processes to occur, such as dissociation, (dissociative) ionization, (dissociative) attachment, recombination and dissociative excitation. Each of these processes is characterized by its own cross-section, σ (E) which is showed overlapping with EEDF in Figure 1.2. The rate constant k of the electronically collisional processes is proportional to the product of EEDF and cross-section, according to the following formula:

$$k = \int E^{1/2} f(E)\, \sigma(E)\, dE$$

The onset of these processes starts at 10 eV or higher, while the EEDF peaks around 1-2 eV. Hence, the tail of the EEDF mainly determines which processes can possibly occur.

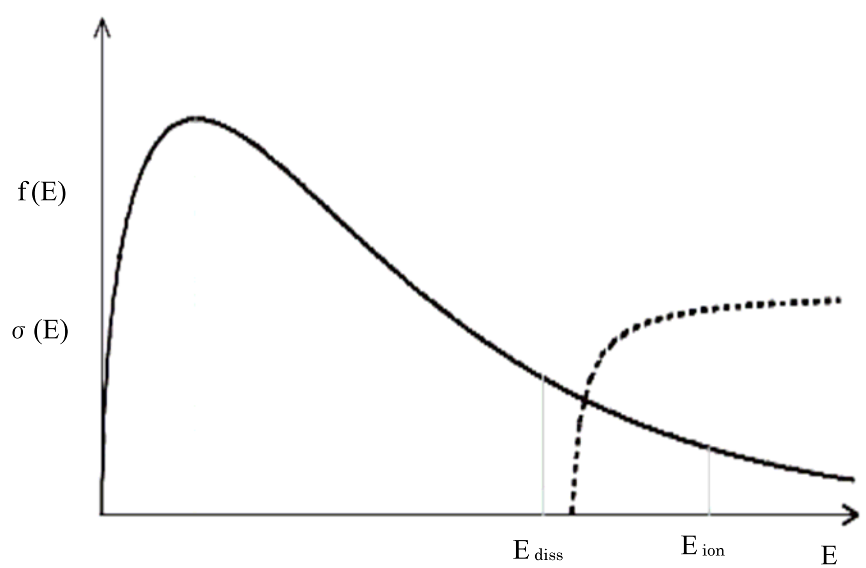

Figure 1.2 Electron energy distribution function and the reactive cross-section. The rate of an electronic reaction is proportional to the product of the two.[9]

1.3. Plasma Polymerization

Starting in the 1960s, scientists have successfully explored the plasma techniques in material science, including plasma polymerization.[10,11] Inspired to the use of plasma polymer as a dielectric film during the early development of microelectronic field at that time, the systematic investigations of plasma polymerization were followed by the rapid advancement of polymer science. Nowadays, the advantages of plasma polymerization have been fully recognized not only in the field of microelectronics but also covering many potential applications in optical field, polymer science, sensors, membrane and surface modification of biomedical materials.[12]

Most of the works corresponding to the plasma polymerization, however, were intended for surface modifications of polymer surface. This is due to the fact that the effects of the plasma do not penetrate more than 100 Å from the surface.[13] Because the bulk of the material is not affected by the treatment, the desirable structural characteristics can be maintained. Polymerization under influence of plasma can be divided into two methods: plasma-state polymerization and plasma-induced graft polymerization. In the last two decades, both of these processes have been utilized to develop macromolecular plasma chemistry, with emphasizing directions to the surface functionalization of polymeric materials and plasma-enhanced synthesis of thin layer of macromolecular structures.[14]

1.3.1. Plasma(-State) Polymerization

Plasma-state polymerization, which is simply so-called by plasma

polymerization, deals with the formation of deposit thin films from gaseous atmosphere containing monomer with the aid of plasma. Plasma enhanced chemical vapor deposition (PECVD) is the synonymous name of this method. The term plasma polymerization is used to emphasize deposition process from organic-based monomers while PECVD is used for depositing films with rather inorganic character. The principle process of plasma polymerization can be explained by the following concept. Upon transfer energy in the plasma through inelastic collisions, the monomers are fragmented into activated species, free radicals and/or their constituent atoms. The activated fragments are recombined and re-arranged by a rapid step growth mechanism, and deposition occurs due to a loss of kinetic energy upon collision of the activated species with the substrates or walls of the reactor. The loss of kinetic energy is due either to a chemical reaction of the species or increased molecular weight.[15] The activated species for film formation come from the gas phase, but the actual film formation proceeds at the substrate surface. Deposited species containing unpaired electrons are highly unstable, and the molecules become highly reactive at the surface of exposed substrates. The repetition of activation/fragmentation and recombination leads to film formation. The advantages of plasma polymerization include the fact that highly cross-linked, pinhole free, thermally and chemically stable, very adherent and conformal thin films can be deposited on most substrates, using a relatively simple one-step coating procedure.[16,17] Furthermore, plasma polymerized films can also be prepared from monomers that cannot be polymerized by conventional chemical techniques such as methane, saturated hydrocarbons and organo-metallics. The structure of deposited

films is not as well defined as that of conventional polymers and still remains as a very complex process that is not quite well understood. However, several groups have reported that the characteristics of plasma-formed films are highly influenced by many different factors such as reactor geometry, input power, frequency, substrate temperature and monomer flow rate.[18-24]

1.3.2. Plasma-Induced Graft Polymerization

In the plasma-induced graft polymerization which is often referred to plasma grafting, activation of substrate surface is initiated by plasma under reactive gas atmosphere followed with the subsequent grafting reaction of vinyl monomers, either in the presence of vapor or liquid phase.[25,26] The effects of plasma treatment on the substrate surface allows determination of maximum concentration of the formed free radicals, while the degree of grafting itself is influenced by grafting parameters such as: monomer concentration, grafting time and graft medium. The following two different mechanisms have been generally used to explain the occurrence in plasma grafting:[27]

(1) The creation of active species on the polymer surface, followed by contact with the monomer:

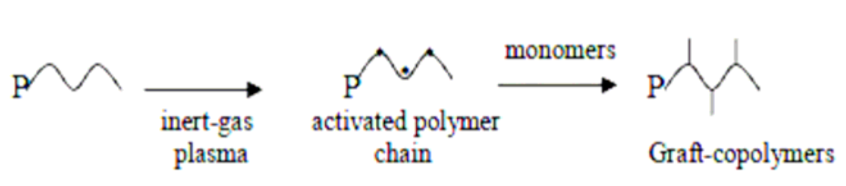

In this mechanism, free radicals are formed on the polymer surface as a result of inert gas plasma treatment. These radicals can either directly initiate grafting or be

converted into peroxide or hydroperoxides by the inclusion of an oxidative gas. These activated peroxides will also initiate grafting in the presence of the monomer species.[28] This method, however, has a potential limitation by side reactions during transport from the reactor into the contacted monomer, which lower the yield.[29]

(2) Direct grafting of the polymer with common or unconventional monomers under "monomer"-plasma conditions:

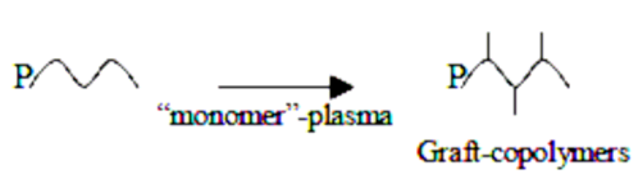

Unlike the previous method, this involves a combined plasma and monomer exposure directly in one step by the use of gaseous monomers in the working gas mixture. The lack of this method is the restriction of monomers with a sufficiently high vapor pressure.[19] However, both of these techniques have shown great advantages over conventional grafting by offering a large range of chemical compounds to be used as monomers, varying thickness of monomer layers, and limited destruction of bulk properties.[18] In this thesis, low pressure cold plasma under air atmosphere was utilized to introduce reactive species on kenaf fiber. These free radicals were allowed to convert to the peroxide after reaction with oxidative air prior to successive graft polymerization.

1.4 Problems in Plasma Polymerization Technique

Non-equilibrium low temperature plasma for plasma polymerization can be

achieved in a wide range of temperatures and pressures. To date, the well established method in low temperature plasma processing is carried out by transferring electrical energy in between two electrodes under reduced pressure in the range of 10 to 1000 Pa. The so-called low-pressure plasma has been come to a great value in fundamental research as well as plasma technology. However, this technique lacks in some points such as the necessity of the vacuum system which leads to the costly operation and the batch processes that are unsuitable for the continuous sequence of manufacturing because the samples needed to be transferred into and out of a vacuum system. Therefore, in order to overcome such problems, recent trends have been focusing on the development of new plasma sources operated at atmospheric pressure with still keeping the characteristic of low temperature.[30] Several numbers of atmospheric pressure plasma sources have been developed for generating non-equilibrium plasma such as conventional dielectric barrier discharge (DBD),[31-33] planar DBD,[34] various types of coronas,[35,36] micro-hollow cathode,[37] direct current,[38] microwave (MW) discharge,[39] and radio frequency glow discharges.[40-43] Some of them have been proved to be utilized for PECVD to effectively deposit thin solid films with characteristics comparable to those films deposited using low pressure modes.[44-46] Major part of this thesis deals with the study in developing a novel atmospheric pressure plasma torch and its application on depositing thin solid films that having characteristic of either organic and inorganic (silicon dioxide) features. The advantages of using this novel torch not only can be operated in atmospheric pressure, thus, solving two shortcomings mentioned above and satisfying the reduced cost requirements, but also can be employed without needing a chamber, hence, capable to

carry out plasma treatment of even complex geometry substrate with no limitation in size.

Low pressure plasma treatment, however, still be engaged in academic or industrial application of plasma. This is due to the specific property of low pressure plasma system to easily generate glow discharge in spite of the type of gases used. Moreover, treatment with the glow discharge results in better properties on substrate surface than filamentary discharge due to the homogeneous character of the discharge. From these points of view low pressure plasma keeps its function in many fields of plasma applications. The low pressure plasma technology has more than 40 years history and has been used in a variety of applications, however, there still exists unsolved problems. Limiting the applications to the polymer treatment, one of the problems should be ascribed to the matter of substrates. If the plasma would be conducted with the purpose only for surface treatment, any kinds of polymer substrates can be processed. However, for the purpose of modification by graft polymerization, the substrate to modify has been mostly in the form of film or textile[47-49] and little attempt have been reported for fibers. Above all fibers, natural fiber, especially plant fiber has not been the substrate for plasma-induced grafting. This is mainly because natural fibers are complex substrates with relatively high lignin content, thus very difficult to proceed the grafting. However, due to its potentially outstanding properties as the filler for environment conscience composite materials, the increase in the use of natural fiber is very rapid.

In this thesis, low pressure plasma has been applied to induce graft polymerization of methyl methacrylate onto natural kenaf fiber. This research was

executed with the purpose of modification the hydrophilic surface of kenaf closer to hydrophobic surface in order to increase the compatibility with the polymer matrix for preparation composite material where the treatment did not alternate the high ratio properties of kenaf fiber. Combination of the plasma surface activation with post-plasma grafting using aqueous solutions is chosen as an environmentally attractive alternative to the use of organic solvents. This technique avoids organic solvents for the graft polymerization, thereby reducing the environmental pollution caused by the production process of highly toxic wastes.

1.5. Aims of This Thesis

The main objective of this works is developing a novel non-equilibrium atmospheric pressure plasma source operated based on argon gas and explores the possibility of using this tool in depositing organic-based thin film and silica-like films. Polymer thin films are great of interest for surface engineering of organic and inorganic substrate surfaces to enhance the substrate's chemical selectivity and modify the surface topology in such areas as chemical sensing, barrier coatings, biotechnology and separation technology. The approach consists in analyzing the gas phase chemistry as well as characterization of deposit films in order to be able to form the relationship between the discharge parameters and deposition properties. This can be fulfilled by performing in situ diagnostic with optical emission spectroscopy (OES), and film characterization with Fourier transform spectroscopy (FTIR), X-ray photoelectron spectroscopy (XPS) and scanning electron microscope (SEM).

The second objective of this thesis is to try the application of low pressure

plasma treatment as a means to induce graft polymerization of vinyl monomer for surface modification of kenaf fiber. The surface modification is needed in order to keep the high aspect ratio of kenaf unchanged as reinforcement for composite material, while the hydrophilicity of the surface was reduced and permanently altered to hydrophobic feature for easy compatibility with polymer matrix.

References

1. Boenig, H. V., Fundamentals of Plasma Chemistry and Technology, Technomic Publishing Co., Inc.: Lancaster, PA (1988).
2. M.A. Lieberman and A.J Lichtenberg, Principles of Plasma Discharges and Materials Processing 2nd Edition, John Wiley & Sons, Inc. (2005).
3. Yasuda, H., Plasma Polymerization, Academic Press Inc.: Orlando, FL (1985).
4. A. Bogaerts, E. Neyts, R. Gijbels, J. van der Mullen, *Spectrochimica Acta Part B*, **57**, 609-658 (2002).
5. B. Chapman, Glow Discharge Processes, Sputtering and Plasma Etching, Wiley, NewYork, U.S.A. (1980).
6. A. Fridman, A. Chirokov and A. Gutsol, *J. Phys. D: Appl. Phys.*, **38**, R1-R24 (2005).
7. V. A. Godyak and R. B. Piejak, *Phys. Rev. Lett.*, **65**, 996 (1990).
8. A. Grill, Cold Plasma in Materials Fabrications From Fundamentals to Applications. IEEE Press, Piscataway, NJ (1994).
9. C. Cavallotti, M. Di Stanislao, S. Carra, *Progress in Crystal Growth and Characterization of Materials*, **48/49**, 123-165 (2004).
10. J. Goodmann, *Journal of Polymer Science*, **44**, 551 (1960).
11. A.P. Bradley, J. P. Hammes, *J. Electrochem. Soc.,* **110**, 15 (1963).
12. Hynek Biederman, Plasma Polymer Films, Imperial College Press (2004).
13. M. V. Bhat, Y. N. Benjamin, *Text. Res. J.*, **69**, 39 (1999).
14. F. S. Denes, S. Monolache, *Progress in Polymer Science*, **29**, 815-885 (2004).
15. H.K. Yasuda, Plasma Polymerization; Chapt 10, Academic Press: Orlando, FL (1985).
16. Rinsch, C. L., Chen, X., Panchalingam, V. Eberhart, R. C., Wang, J. H.; Timmons, R. B., *Langmuir* **12**, 2995 (1996).
17. W.J. van Ooij, F.J. Boerio, A. Sabata, D.B. Zeik, C.E. Taylor, S.J. Clarson, *J. Test. Eval.*, **23**, 33 (1995).
18. Yasuda, H.; Hirotsu, T., *J. Appl. Polym.*, **21**, 3167 (1977).
19. Yasuda, H.; Hirotsu, T., *J. Polym. Sci. Polym. Chem. Ed.*, **16**, 313 (1978).

20. Yasuda, H.; Hirotsu, T., *J. Polym. Sci. Polym. Chem. Ed.,* **16**, 2587 (1978).
21. Morita, S.; Bell, A. T.; Shen, M.*, J. Polym. Sci. Polym. Chem. Ed.*, **17**, 2775 (1979).
22. E. Kay, L.L. Levenson, W.J. James, R.A. Auerbach, *J. Vac. Sci. Technol.*, **16**, 359 (1979).
23. Ohkubo, J.; Inagaki, N., *J. Appl. Polym.*, **41**, 349 (1990).
24. H. Biederman; D. Slavinska, *Surf. Coat. Technol.*, **125**, 371 (2000).
25. I. Gancarz, G. Pozniak, M. Bryjak and A. Frankiewicz, *Acta Polym.*, **50**, 317 (1999).
26. K. Kato, E. Uchida, E.T. Kang, Y. Uyama, Y. Ikada, *Prog. Polym. Sci.*, **28**, 209 (2003).
27. C.I. Simionescu and F. Denes, *Cellulose Chem. Technol.*, **14**, 285 (1980).
28. C.I. Simionescu, F. Denes, M. M. Macoveanu and I. Negulescu, *Makromol. Chem. Suppl.*, **8**, 17 (1984).
29. C. Oehr, M. Muller, B. Elkin, D. Hagemann, U. Vohrer, *Surface and Coating Technology*, **116-119**, 25-35 (1999).
30. A. Schutze, J. Y. Jeong, S. E. Babayan, J. Park, G. S. Selwyn, and R. F. Hicks, *IEEE Transactions on Plasma Science*, **26**, 1685 (1998).
31. J. Salge, *Surface and Coatings Technology*, **80**, 1-7 (1996).
32. A.P. Napartovich, *Plasmas and Polymers*, **6**, 1-14 (2001).
33. U. Kogelschats, B. Eliasson, W. Egli, *J. Phys IV*, **C4**, 47 (1997).
34. J. Engemann, D. Korzec, *Thin Solid Films*, **442**, 36 (2003).
35. J. Chen, J.H. Davidson, *Plasma Chem. Plasma Process.*, **22**, 199 (2002).
36. K. Yan, E.J.M. van Heesch, A.J.M. Pemen, P.A.H.J. Huijbrechts, *Plasma Chem. Plasma Process.*, **21**, 107 (2001).
37. R.H. Stark, K.H. Schoenbach, *Appl. Phys. Lett.*, **74**, 3770 (1999).
38. O. Goossens, T. Callebaut, Y. Akishev, A. Napartovich, N. Trushkin, C. Leys, *IEEE Transactions on Plasma Science*, **30**, 176 (2002).
39. A. Pfuch, R. Cihar, *Surface and Coatings Technology*, **183**, 134-140 (2004).
40. S.D. Anghel, *IEEE Transactions on Plasma Science*, **30**, 660 (2002).

41. Y. Mori, K. Yoshii, K. Yasutake, H. Kakiuchi, H. Ohmi, K. Wada, *Thin Solid Films*, **444**, 138 (2003).
42. L. O'Neill, L.-A. O'Hare, S. R. Leadley, A. J. Goodwin, *Chemical Vapor Deposition*, **11**, 447 (2005).
43. J. Park, I. Henins. H.W. Herrmann and G.S. Selwyn, *Appl. Phys. Lett.*, **76**, 288 (2000).
44. Y. Sawada, S. Ogawa and M. Kogoma, *J. Phys. D: Appl. Phys.*, **28**, 1661 (1995).
45. X. Zhu, F.A. Khonsari, C.P. Etienne, M. Tatoulian, *Plasma Processes and Polymers*, **2**, 407-413 (2005).
46. H. Kakiuchi, Y. Nakahama, H. Ohmi, K. Yasutake, K. Yoshii, Y. Mori, *Thin Solid Films*, **479**, 17-23 (2005).
47. B. Gupta, J. G. Hilborn, I. Bisson, P. Frey, *J. of Appl. Polym. Sci.*, **81**, 2993-3001 (2001)
48. Zubaidi, Toshihiro Hirotsu, *J. of Appl. Polym. Sci.,* **61**, 1579-1584 (1996).
49. Noureddine Abidi, Eric Hequet, *J. of Appl. Polym.*, Sci., **93**, 145-154 (2004).

CHAPTER II

Development and Characterization of a Novel Non-equilibrium Atmospheric Pressure Plasma Torch

Abstract

A novel non-equilibrium atmospheric pressure plasma torch has been developed. The properties of the discharge have been characterized both in electric and spectroscopic measurements. Electrically, the plasma appeared to be a type of glow discharge showing smooth sinusoidal discharge current. Emission spectroscopy of helium (He) and argon (Ar) plasma jet flowing out in open air indicated the diffusion of air components such as nitrogen, oxygen and moisture into the jet leading to the appearance of their emission together with the emission of electronically excited He or Ar. The measurements of plasma jet temperature clarified that the jet is as cold as room temperature. The length of plasma jet was influenced by the applied voltage and gas flow rate. The proper condition to generate the jet as long as 40 mm was found to be 3.0 L/min of He gas feed under the applied voltage of 5.0 kV with 68.0 kHz frequency.

Introduction

Recently, there has been increased interest and development in non-equilibrium (non-thermal) plasma processes working at atmospheric pressure. This is motivated by the growing requirements of new plasma technology that can treat any objects without being restricted by the size or the shape and that can allow the continuous in-line plasma processing of materials. The plasma treatments operated under reduced pressure loose their capabilities to overcome such needs, besides the expensive cost to provide the vacuum systems. A number of novel non-equilibrium atmospheric pressure plasma sources have been developed, for instance the one atmosphere uniform glow discharge plasma (OAUGDP),[1] the atmospheric pressure plasma jet (APPJ),[2-4] the micro beam plasma generator,[5] and plasma needle[11] besides the conventional corona[6,7] and the dielectric barrier discharge (DBD).[8-10] Most of these plasma devices use helium (He) gas as the working gas and have shown the potential for replacement of traditional low pressure plasma system. The utilization so far has been proved effectively in plasma applications, such as sterilization, decontamination, cleaning, etching, surface treatment and film deposition. Among of these sources, plasma jet type can become a powerful tool owing to its capability of operating without any chamber, thus no limitation on the substrate size and dimensions.

We have successfully developed a new plasma jet source based on the DBD type discharge. We named it “CAPPLAT”, Cold Atmosphere Pressure Plasma Torch.[19] It can generate a non-equilibrium plasma jet with the length of 40 mm using He as the working gas. However, the plasma jet generated by it has a diameter less than 3 mm which is not always suitable for the surface treatment processing.

Therefore another type of CAPPLAT has been developed in this chapter of which plasma generation is based on the surface discharge. This torch is operated either with He or in argon (Ar) as the working gas. The usage of argon gas to sustain the discharge become very necessary to open a wide range of chemistry, besides the economical benefit of its cost compared to helium gas. Moreover, the temperature of the torch effluent is much closer to room temperature than other plasma jet, thus more suitable for plasma-mediated treatment of even temperature-sensitive materials. In this chapter, a configuration of plasma torch will be described and the characteristics of the torch discharge are explained on the basis of electrical diagnostic and light emission study.

Experimental

Plasma Torch Configuration and Experimental

Figure 2.1 shows the schematic drawing of the non-equilibrium atmospheric pressure plasma torch. It consists of stainless pipe which is covered coaxially with a silicone tube of 2 mm thick and a stainless belt of 20 mm wide is placed around the silicone tube near its end. The stainless pipe of 4 mm inner diameter has a total length about 10 cm and is connected to the pulse-modulated high voltage power supply (Haiden Lab, PHF-2K), while the stainless belt is grounded. The operational voltage is in the range of some kV at a medium frequency range (30 - 68 kHz). The working gas (He or Ar) was supplied to flow through the stainless pipe at a typical rate of 3 L/min, unless stated otherwise. Electrical diagnostic was performed by measuring the discharge current using a current probe (Keyence Data Acquisition System, NR - 350)

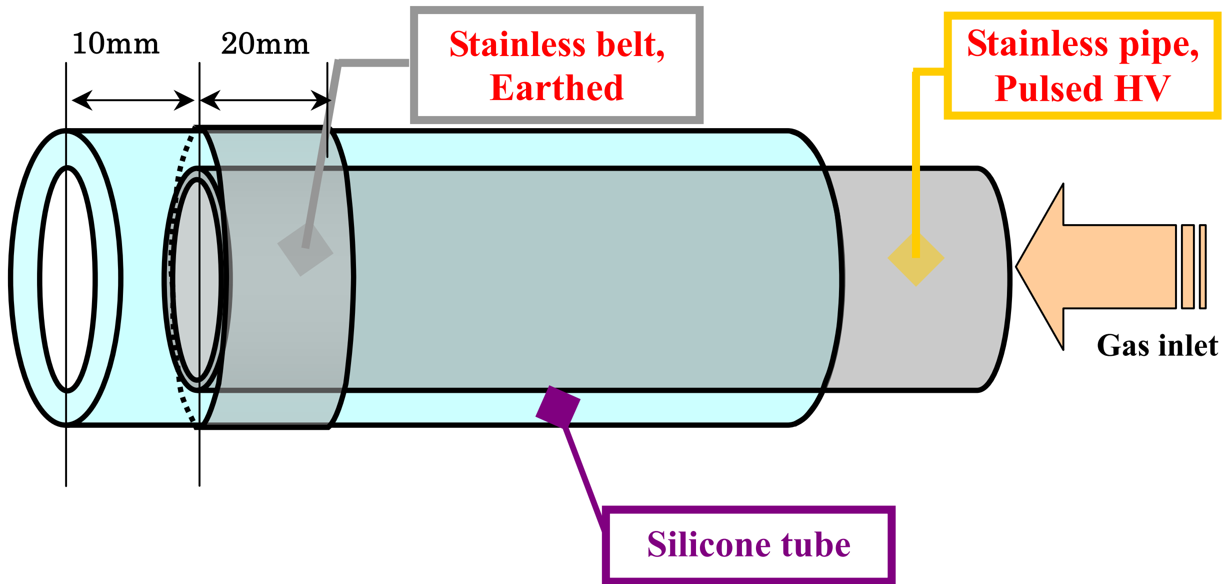

Figure 2.1. Schematic drawing and picture of the plasma torch.

through a series connection of 15 kΩ resistor with the grounded electrode. Schematic diagram of the circuit of the current discharge measurement is shown in Figure 2.2. The results were recorded on a computer-based oscilloscope.

In order to estimate the active species in the plasma jet, emission spectra were observed by using a Multiband Plasma-Process Monitor (MPM, Hamamatsu Photonics C7460). The spectra were collected in the range 200-950 nm through an optical fiber equipped perpendicularly to the plasma jet. Monitoring and data acquisition of the emission spectra were carried out by a PC. In addition, the gas temperature of the plasma jet was measured by either an infrared thermometer or a thermocouple.

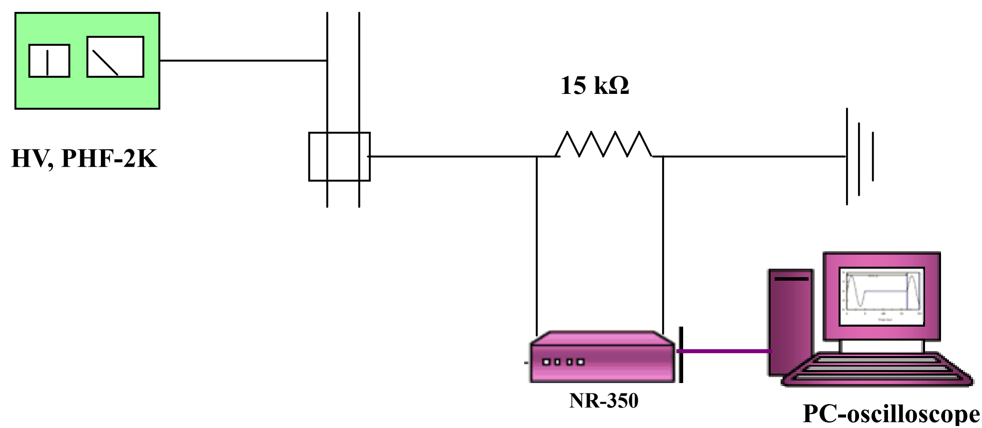

Figure 2.2 Circuit scheme for measurement of the discharge current.

Results and Discussion

Electrical Diagnostic

Since the founding of Kanazawa et al.[12-15] that diffuse (homogeneous) plasma can be generated at an atmospheric pressure with some requirements, such as using He gas, covering electrodes with dielectrics, and powering the discharge with a high frequency source, this invention has motivated the other groups to investigate another type of atmospheric pressure glow discharge using He as the basic gas.[16-17] However, the high cost of He and gas recovery systems deliver another problems to the widespread applications of plasma treatment using He-based glow discharge. Therefore, our laboratory has taken a challenge and successfully developed a novel non-equilibrium atmospheric pressure plasma torch which can be operated with less expensive Ar gas.

Preliminary study of using this torch revealed that 68.0 kHz is the optimal frequency to generate the Ar plasma jet. Therefore, most of the works related plasma ignitions were carried out with this frequency. The typical oscilloscope patterns of time-dependent current in discharge operated with He and Ar are shown in Figure 2.3. Almost smoothed sinusoidal curves observed for both working gases without any spiky lines, which indicates that the discharges are homogeneous glow. However, visual observation gave recognition to rather filamentary micro-discharge in typical Ar plasma jet while the He plasma kept glow discharge. On the other hand, the impulse response of the discharge current of the circuit shows twice damped oscillations of applied voltage with 14.7 μs cycle. This might be due to the capacitive

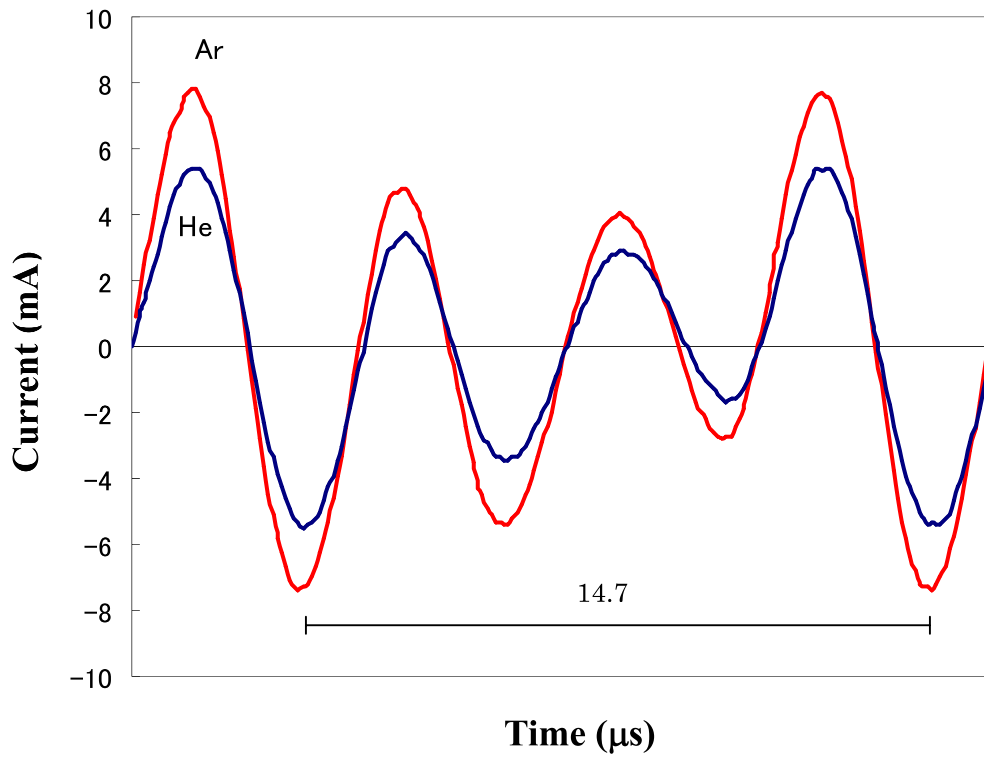

Figure 2.3. Oscillogram of the current pulse of the He and Ar plasma torch.

coupling of the circuits with dielectric silicone and discharged gas. It can also be observed in Figure 2.3 that the sinusoidal of the curves are almost identical for the two systems, however, the inconsistency of their amplitudes are obvious. The discharge current of Ar plasma is larger than that of the He plasma. This means that, compared to He plasma, more energy transfer occurred in Ar plasma to dissociate and excite the working gas to produce higher density of active species. In order to verify the conclusion, the optical emission spectroscopy analyses were performed.

Optical Emission Spectroscopy (OES)

OES has been used to detect plasma composition by observing the electronically excited species and their intensities in the discharges generated by He and Ar plasma torch. The spectra obtained from those plasmas are shown in Figure 2.4. The spectrum of He plasma exhibits emission lines corresponding to the He neutral (588-728 nm), atomic oxygen (777 and 845 nm), a group of N_2 emissions in the form of second positive system (SPS) at 316, 337, 358, 380 and 406 nm and first negative system (FNS) at 391, 428 and 471 nm and OH (at 306 nm)[18,19]. The existed emissions of OH and nitrogen generally could be ascribed to the presence of water vapor from air atmosphere, while oxygen might be because of the same reason like above or come from the silicone tube. Considering the dominated intensity of N_2 species in He plasma, those emissions are plausibly the results of energy transfer from metastable rare gases to the components of air. In the case of Ar plasma, very intense excited Ar is dominant at the wavelength from 699 to 922 nm. In addition, the lines of OH and N_2 groups were also detected as a consequence of the discharge in open air

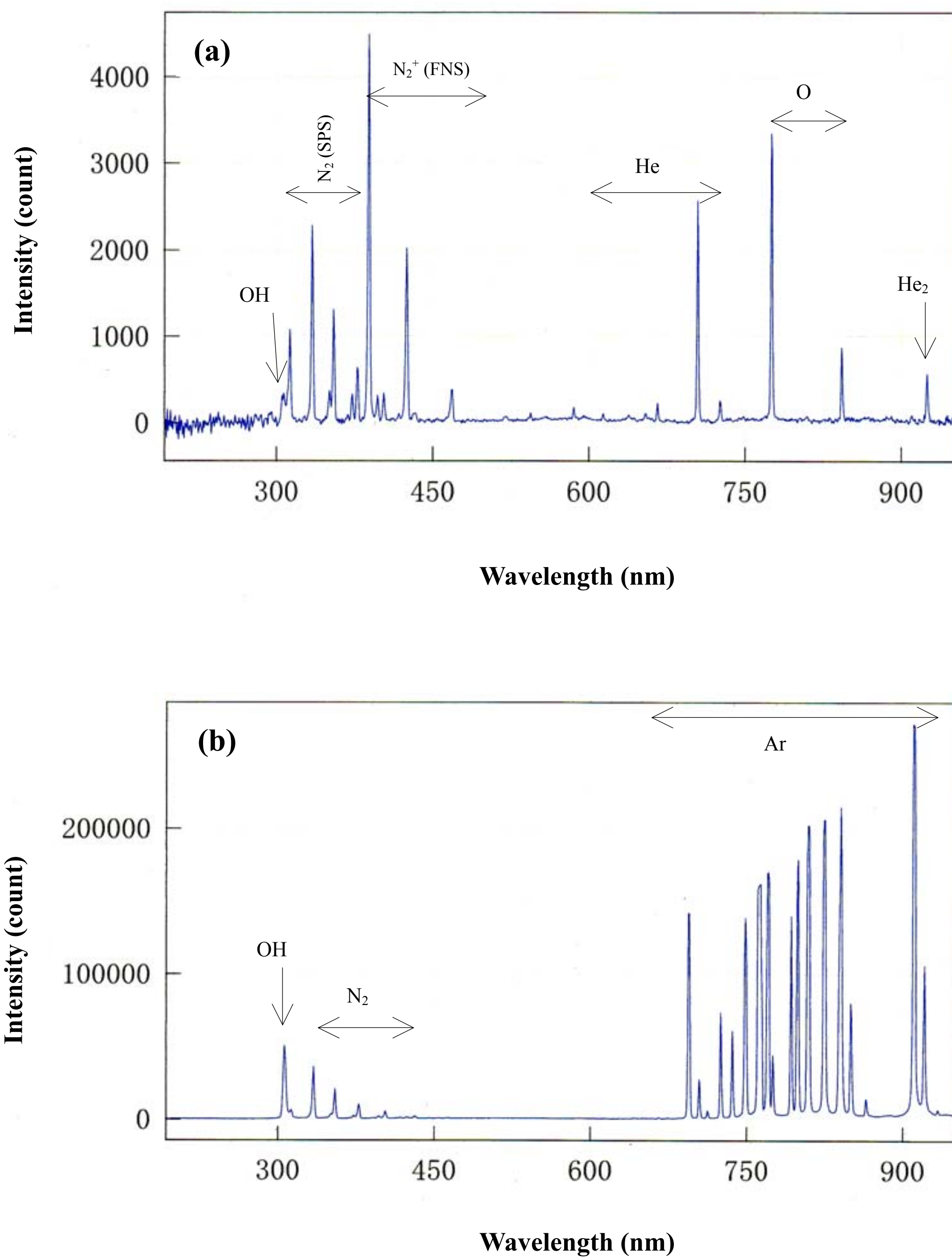

Figure 2.4 Spectra of He (a) and Ar (b) plasmas, operated in open air.

system. It is noteworthy that the intensities of active species in Ar plasma are more than 20 orders in magnitude of those in He plasma. This is in accordance with the previous electrical diagnostic that the more energy transfer takes place in Ar plasma than in He plasma at the same applied voltage.

It is generally known that He can generate glow discharge in atmospheric pressure and have been used by showing better yields than filamentary-based discharge in many practical applications. From the results mentioned above, it is shown that the density of active species in Ar plasma is much higher than in He plasma. As the emission intensities of He and Ar plasma can be related to the density of electrons with energy higher than their excitation thresholds[20,21], this will lead to the open new plasma chemistry including higher density of 'hot' electron owned by Ar plasma. However, the filamentary characteristic of Ar plasma will suppress the utilization in applications. If the diffuse plasma characteristic can be provided in Ar-based plasma, it will be very useful and many advantages could be expected. During the experiments with Ar plasma, the author found that addition of a small amount of nitrogen gas could change the filamentary character of the Ar plasma closer to the feature of the homogeneous discharge. OES of the Ar plasma with several amount of admixed N_2 gas is given in Figure 2.5. This plasma generation was carried out in a glass chamber in order to avoid the possible contaminant reaction of any gases in the open air with the plasma. Inclusion of 0.05 L/min of N_2 to 3 L/min of Ar feed gas yields the emission of a group of second positive system (SPS) of neutral N_2 without spectrum of the first negative system (FNS). Furthermore, the intensity of Ar emission lines is highly reduced. Besides, the color of the plasma also changed from

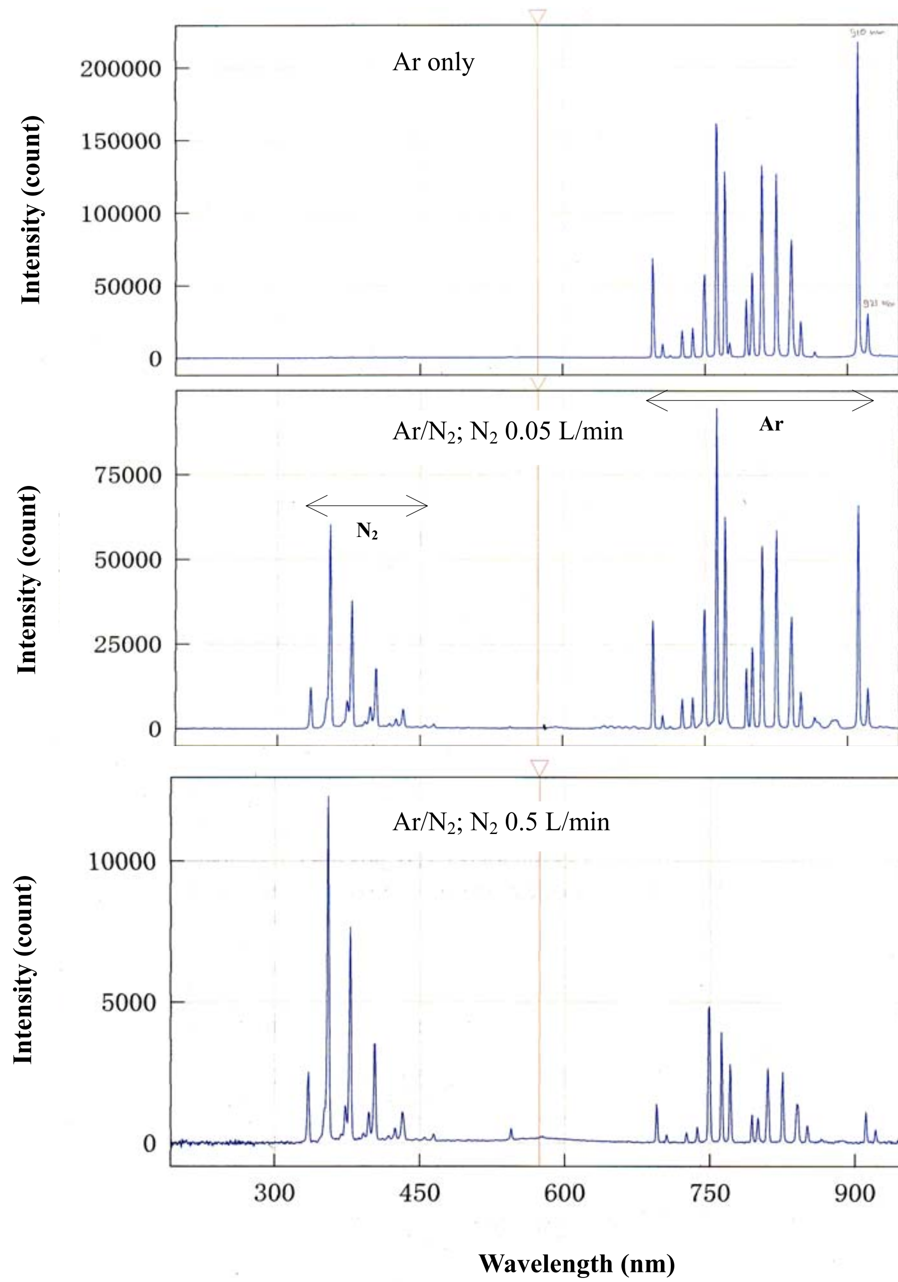

Figure 2.5 Emission spectra of Ar and Ar/N_2 plasma at different amount of N_2 rate.

light blue to violet blue. Increasing the amount of N_2 admixed to the higher amount caused the domination of the N_2 emission over Ar emission. Raising the N_2 flow rate over 0.7 L/min extinguished the plasma. Selective excitation of nitrogen species occurred because transfer energy of Ar excitation threshold ($E_{Th} \approx 13.5$ eV) is only sufficient to excite the SPS N_2 ($E_{Th} \approx 11$ eV) and not enough for exciting FNS N_2^+ which having energy threshold of 18.7 eV.

Plasma Temperature

The measurement of gas temperature of the non-equilibrium atmospheric pressure plasma jet was carried out by two methods. First, the jet effluent along the axis at its end was directly measured using a thermocouple. Secondly, a piece of silicon wafer was placed at 2 cm from the torch end where the plasma jet stroke the wafer directly, and the infrared thermometer was shot on that place every minute. The measurements were conducted at surrounding temperature of 25℃. By using these methods, both information of gas temperature and the effect to the substrate temperature would be obtained. It was found that both methods yielded a similar result for He and Ar plasma. The increase in temperature by time extension is summarized in Figure 2.6. The experimental conditions were 3 L/min of gas feed, 3.5 kV of applied voltage and 68.0 kHz in frequency. From the same starting point, it appears that the increment of temperature for Ar plasma is more than that for He plasma, however, those plasmas find their saturated temperature at the same period of 10 min. It needs to be pointed out from this experiment that the temperature of the

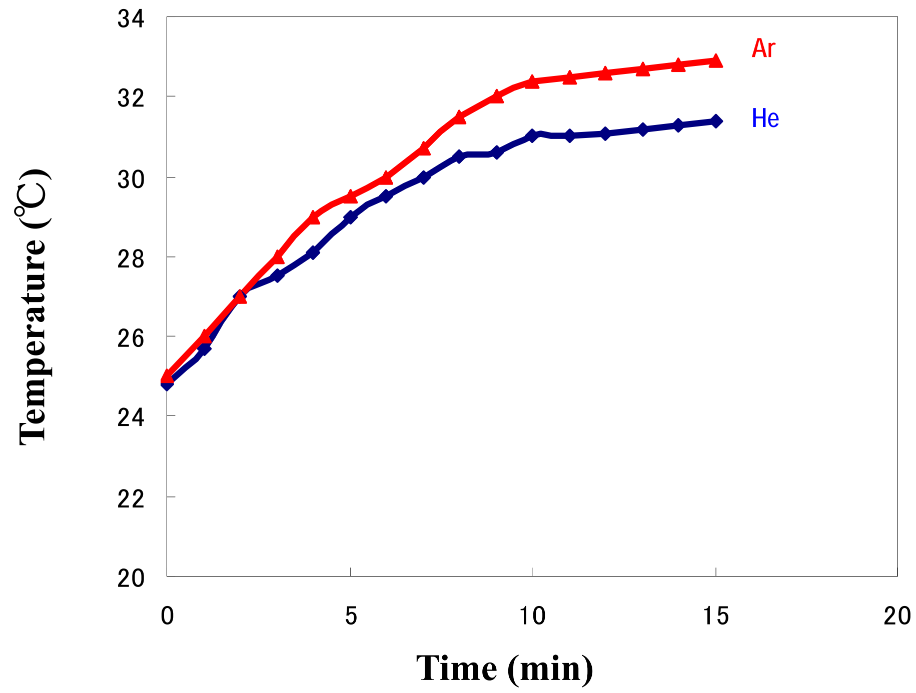

Figure 2.6. Temperature increment profile of the He and Ar plasma torch by the time.

present plasma jet is much closer to room temperature than any other design of plasma jet.[2,3] It becomes very clear therefore that the present novel plasma torch has a great possibility to broaden its application, not only to change the surface properties of polymers, but also for surface modification of temperature-sensitive materials or even can be applied on tissue engineering. The main reason why the gas discharge still keeps low in temperature is because of the usage of pulsed power supply. The characteristic of the pulsed power is its capability to switch the power on and off repeatingly thousands times during a second. Due to its discontinuity of cycling power, the pulsed power can be expected to provide plasma temperature stay low.

Verification of low temperature of the plasma jet was also performed by simply touching it by the hand, as showed in Figure 2.7. The He glow discharge can strike the bare human skin without causing harm effect. This is because the transferring of several kilovolts pulsed power to the working gas only to excite the light electrons and leave the heavy neutral particles unaffected.

Plasma Jet Length Dependency

It is valuable to understand the controlling factors of the plasma jet length because it will bring benefits to the practical use of the present plasma torch. An adequate length of plasma jet might be very important so as to enable various and useful chemical reactions on the substrate surface. Control of the jet length in this study has been performed through examining the influence of applied voltage and flow rate of feed gas. He gas was used to execute the initial trials. Figure 2.8 shows the effect of applied voltage on plasma jet length at different He flow rate using

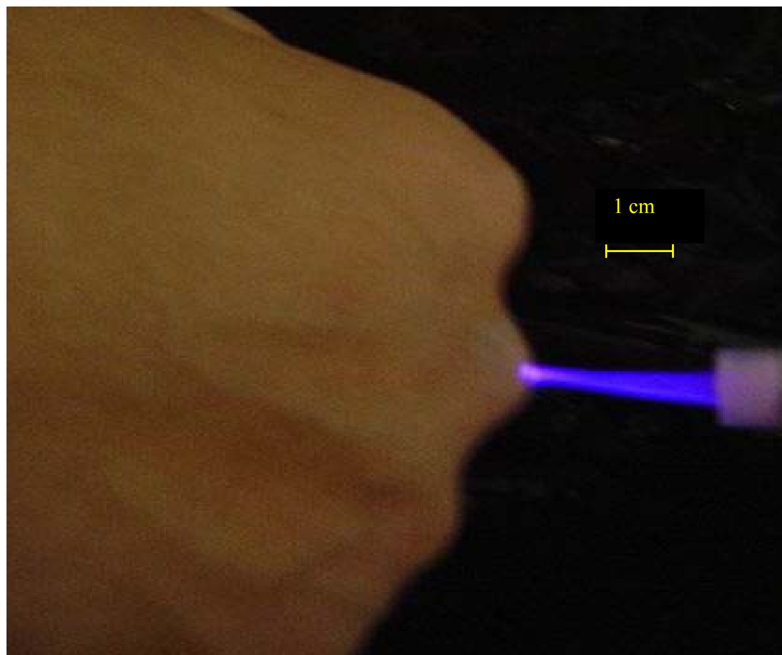

Figure 2.7 Glow He plasma torch in contact with human bare skin.

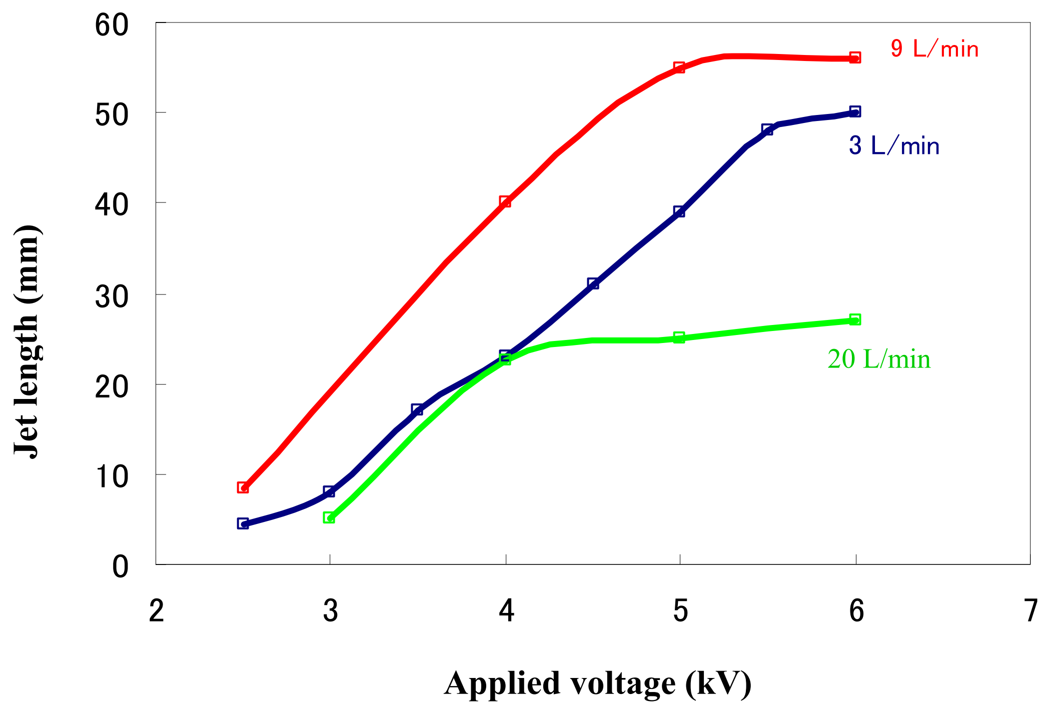

Figure 2.8 Effect of applied voltage on plasma torch length at different He flow rate.

frequency of 68 kHz. It is obvious that raising the applied voltage yields increasing of jet length for all feeding rate. This is reasonable as the strength of applied electrical field will determine the amount of charged particles. On the contrary, increasing the flow rate of He gas from 9 L/min to 20 L/min results in decrease of the jet length. This fact might be attributed to the shortening of contact time of the fed to the electrode surface owing to its high gas fluid velocity. Practically, the use of large amount of He is not desirable because of higher cost for operation. The flow rate of 3 L/min seems to be the necessary and sufficient stream of He gas to sustain the plasma jet. This feeding rate was therefore adopted to generate the plasma jet for its application to the deposition of thin films in the subsequent chapters.

Conclusion

This chapter describes development and characterization of `Cold Atmosphere Pressure Plasma Torch` or CAPPLAT. The design was adjusted in which the stainless belt was placed around the silicone tube covered stainless pipe near its end for the ease of generating with He and Ar as the working gas. Electrically, the discharge was a type of homogenous glow, though visually Ar plasma rather showed filamentary. From the OES results of the plasma jet, the presence of O˙, OH˙ and various of system of N_2 excited species was confirmed when the torch was carried out in open air. The temperature of plasma jet was found to be lower than 35℃. The length of plasma jet was influenced by the applied voltage and gas flow rate.

References

1. R.B. Gadri, J.R. Roth, T.C. Montie, et.al., *Surf, Coat. Technol.*, **131**, 528, 2000.
2. J.Y. Jeong, S.E. Babayan, V.J. Tu, J. Park, I. Henins, R.F. Hicks and G.S. Selwyn, *Plasma Source Sci. Technol.*, **7**, 282-285, 1998.
3. S.E. Babayan, J.Y. Jeong, V.J. Tu, J. Park, G.S. Selwyn and R.F. Hicks, *Plasma Source Sci. Technol*., **7**, 286-288, 1998.
4. V.J. Tu, J.Y. Jeong, A. Schutze, S.E. Babayan, G. Ding, G.S. Selwyn and R.F. Hicks, *J. Vac. Sci. Technol. A*, **18**, 2799, 2000.
5. H. Koinuma, H. Ohkubo and T. Hashimoto, *Appl. Phys. Lett*, **60**, 816, 1992.
6. Van Brunt R.J., *IEEE Trans. Dielectr. Electr. Insul.*, **1**, 761-784, 1994.
7. K.L. Mittal and A. Pizzi, eds., Adhesion Promotion Techniques, Marcel Dekker, NY 1999.
8. T. Yokoyama, M. Kogoma, S. Kanazawa, T. Moriwaki and S. Okazaki, *J. Phys D: Appl. Phys.*, **23**, 374, 1990.
9. F. Massines, A. Rabehi, P. Decomps, R.B. Gadri, P. Segur and C. Mayoux, *J of Appl. Phys.*, **83**, 2950, 1998.
10. S.F. Miralai, E. Monette, R. Bartnikas, G. Czeremuszkin, M. Latreche and M.R. Wertheimer, *Plasmas and Polymers*, **5**, 63, 2000.
11. I.E. Kieft, E.P v d Laan and E. Stoffels, *New J. of Phys.*, **6**, 149, 2004.
12. S. Kanazawa, M. Kogoma, T. Moriwaki and S. Okazaki, *J. Phys D: Appl. Phys.*, **21**, 838, 1988.
13. S. Kanazawa, M. Kogoma, S. Okazaki and T. Moriwaki, *Nucl. Instrum. Meth. Phys.Res. B*, **37/38**, 842, 1989.
14. S. Okazaki, M. Kogoma, M. Uehara and Y. Kimura, *J. Phys D: Appl. Phys.*, **26**, 889, 1993.
15. Y.Sawada, S.Ogawa, M.Kogoma, *Journal of Adhesion*, **53** [3-4], 173 (1995)
16. F. Massines, P. Segur, N. Gherardi, C. Khamphan, A, Richard, *Surf. Coat Technol.*, **174-175**, 8-14 (2003).
17. S. Martin, F. Massines, N. Gherardi, C. Jimenez, *Surf. Coat Technol.*, **177-178**, 693-698 (2003).

18. R.W.B. Pearse, A.G. Gaydon, The Identification of Molecular Spectra. Fourth Edition, Chapman and Hall, 1976.
19. A. Kuwabara, S. Kuroda, H. Kubota, *Plasma Processes and Polymers*, **2** (4), 305-309, 2005.
20. R. Lamendola and R. d'Agostino, *Pure & Appl. Chem.*, **70** (6), 1203-1208, 1998.
21. F. Palumbo, P. Favia, M. Vulpio, R d'Agostino, *Plasmas and Polymers*, **6** (3), 163-174, 2001.

CHAPTER III

Poly(methyl methacrylate) Films Deposited via Non-equilibrium Atmospheric Pressure Plasma Polymerization with Using Argon as the Working Gas

Abstract

A non-equilibrium atmospheric pressure plasma torch using argon (Ar) for sustaining plasma has been developed and it was used to deposit the plasma polymerized methyl methacrylate (PPMMA) films. The chemical structure and composition of the films obtained were examined by FT-IR and XPS analyses. It was found that when raising the concentration of vaporized monomer to a certain level into the plasma, the plasma transitioned from a filamentary to the glow-like discharge, resulting in a high retention of monomer structure. Since the optical emission spectroscopy (OES) study of the plasma did not show any new excited species formed at higher concentrations of monomer, it is clear that the fragmentation degree of the monomer in the plasma phase was quite low.

Introduction

Previous chapter has described the configuration of the novel non-equilibrium atmospheric pressure plasma torch together with its electrical characteristic and optical properties of the discharge. This chapter investigates the application of the torch for deposition of organic film. Plasma polymerized organic thin films have been received a great deal of interest because of their unique characteristics such as: pinhole-free, structurally cross-linked, insoluble and highly adhered to different substrate surfaces. They can potentially offer many practical applications in the field of mechanics, electronics and optics.[1] Of particular interest are the plasma polymerized methyl methacrylate (PPMMA) films, which have been used as dry electron-beam resist,[2] membranes for gas separators, humidity sensor and optical devices such as wavelength transformer.[3,4,5]

Spin coating is a physical process that is generally known to be able to produce thin films from polymer solution with full retention of their functionalities. However, it is very useful and many advantages would be obtained if the polymer film can be deposited using plasma polymerization, due to its characteristic of one-step process, avoiding solvent usage and no volatiles involved. Moreover, the latter process allows deposition of films with the thickness from nano to micrometer level. If the monomer fragmentation in the plasma-mediated process can be controlled in order to gain polymer thin film with full retention of its functional groups, plasma polymerization method would provide the compliment technique to spin-on coating.

The low pressure plasma assisted processes are the well-established and become commonly used methods for the deposition of polymer-like films. However,

the necessity of expensive vacuum systems is the biggest shortcoming of these processes in industrial applications besides the limitation to the batch system processes. Therefore, to overcome these disadvantages, considerable efforts are made in developing alternative techniques. The non-equilibrium atmospheric pressure plasmas are one of the most promising methods to deposit polymer films in a more flexible, reliable, less expensive and continuous way of treatment. Several types of non-equilibrium atmospheric pressure plasma sources have been successfully used for depositing films, and they included atmospheric pressure (AP) dielectric barrier discharge (DBD)[6-11] as the most commonly used atmospheric pressure discharge, AP Plasma Jet, [12-14] and AP plasma chemical vapor deposition (AP-PCVD).[15-16] However, most of them have been using helium (He) as the working gas to generate the plasma. If the plasma could be generated with using argon (Ar) as the working gas, it would bring a great benefit to the technique, because Ar is much less expensive than He and also because the Ar plasmas have better energy transfer efficiency than the He plasmas under the same working conditions.[17] We have successfully developed a non-equilibrium atmospheric pressure plasma torch in which the plasma can be generated either in He or in Ar gas. For the applications in material processing, we explore to deposit organic thin film using this system.

The present study reports the plasma polymerization of methyl methacrylate by non-equilibrium atmospheric pressure plasma torch with using Ar as the working and carrier gas. It will be shown that the deposited PPMMA films are chemically and spectroscopically similar to the conventional poly(methyl methacrylate) (PMMA) synthesized by traditional chain polymerization.

Experimental Part

Materials

The films were deposited either on silicon wafers for XPS analyses or on KBr disks for FT-IR measurements. The substrates were cleaned with acetone under ultrasonic condition prior to the plasma polymerization. Methyl methacrylate (MMA) monomer (Wako Chemicals Co.) was used as the organic precursor after purification through vacuum distillation.

Plasma Polymerization

In order to avoid the direct contact with the process exhaust which may contain hazardous gases, the novel torch has been housed with a reactor and safety outlet portion. The schematic diagram for the non-equilibrium atmospheric pressure plasma polymerization is shown in Figure 3.1. High voltage power supply (Haiden Lab. PHF-2K) was connected to the stainless pipe (inner diameter = 4 mm) electrode, which was embedded in the center of a perforated silicone stopper allowing the gas to flow through. The stopper was inserted into a glass vessel to make the chamber sealed from the ambient air. The exhaustion of gas was done through the vent on the outer side of the silicone stopper. The stainless tape electrode that circled the outer part of the stopper was connected to the ground. Gas mixture consisted of 3.0 L/min of Ar as the working gas and the admixed monomer gas, which was vaporized by passing another Ar tube through the room temperature MMA vessel. This mixture was allowed to flow in through the inlet pipe, and the plasma was ignited by using an electric source at a fixed frequency of 68.0 kHz. The plasma was generated

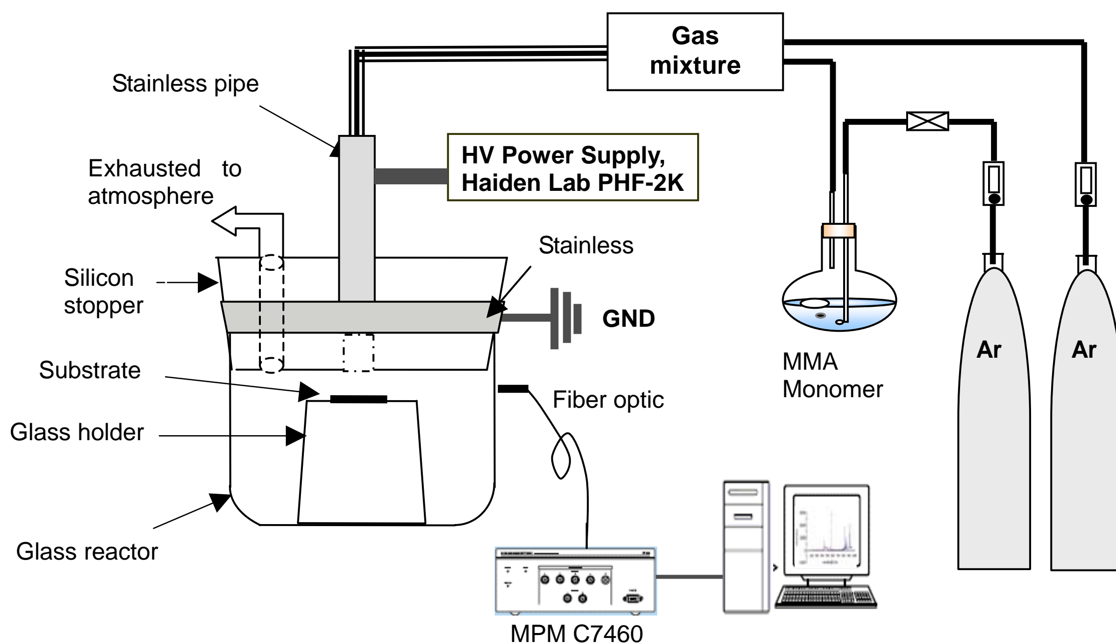

Figure 3.1. Schematic diagram for non-equilibrium atmospheric pressure plasma polymerization experiment set-up.

downstream to the substrate which was positioned along as 2.5 cm distance from the pipe end. The film deposition was carried out for 10 min under various conditions of carrier gas flow rate and the applied voltage. The characteristic of plasma was examined by OES, and the as-deposited PPMMA films were characterized by FT-IR and XPS. OES measurements were performed perpendicularly to the downstream discharge with a Multiband Plasma-Process Monitor (MPM, Hamamatsu Photonics C7460). The emission spectra from the plasma source were acquired through the equipped optical fiber in the range of 200-950 nm. FT-IR analyses were performed to examine the structure of PPMMA films. Transmission mode was used for FT-IR measurements on a Jasco FT-IR-8000 spectrophotometer with 64 scans at 4 cm^{-1} resolution. XPS measurements were carried out on a Perkin Elmer PHI Model 5600 ESCA instrument, using a monochromated Al X-ray source. The binding energy scale was calibrated by setting the C1s peak at 285 eV. The high resolution scan (0.25 eV resolution) spectra of C1s region were also measured, and the obtained spectra were deconvoluted using the curve fitting program of MultiPak V.6.1A.

Results and Discussion

Gas-phase Chemistry

The typical Ar plasma at atmospheric pressure consists of many whitish light-blue streamers leading to the inhomogeneous discharge, which is inexpedient for plasma polymerization. However, the discharge behavior was changed when the vaporized MMA monomer in 0.3 L/min Ar carrier gas was added to the Ar plasma. It gave rise to a pale purple non-filamentary discharge which resulted in glow-like

plasma. It is generally known that the addition of gases such as a halogen, nitrogen or organic molecules can quench or may extinguish the argon glow discharge plasma due to efficient energy transfer from Ar metastables to foreign atoms or molecules.[18] Accordingly, in the present system, the addition of MMA monomer to the atmospheric pressure Ar plasma made a change in the discharge behavior from filamentary to the glow-like one owing to this quenching effect.

Optical emission spectroscopy (OES) was performed to determine the nature of excited species in the Ar plasma with and without the addition of MMA monomer. Shown in Figure 3.2 are the spectra lines obtained from the pure Ar plasma and the Ar plasmas containing various concentration of the admixed monomer, which were obtained by varying the flow rates of the Ar carrier gas. It can be observed from OES of the pure Ar plasma that the spectra lines of the neutral Ar atoms appear strongly in the range of 695 – 921 nm. These lines are in agreement with the spectral Ar lines detected in either an atmospheric pressure barrier discharge,[19] or in that from hollow cathode discharge under 1 torr. [20] When the vaporized monomer was introduced by flowing Ar gas with a flow rate of 0.1 L/min, apart from the Ar lines of Ar which seemed unchanged in emission intensity, a group of low-intensities lines due to CH (431 nm) and CO (519 nm) species[21] was found in the region between 350-520 nm. This indicates that the concentration of MMA in 0.1 L/min Ar gas added to the Ar plasma is too low to give a certain cooling effect to the Ar plasma, and as a result, a high degree of monomer fragmentation has been occurred in the plasma bulk due to the interaction of the high energy electrons with precursor molecules. Increasing the concentration of monomer by flowing 0.3 L/min Ar gas did not yield the new lines of

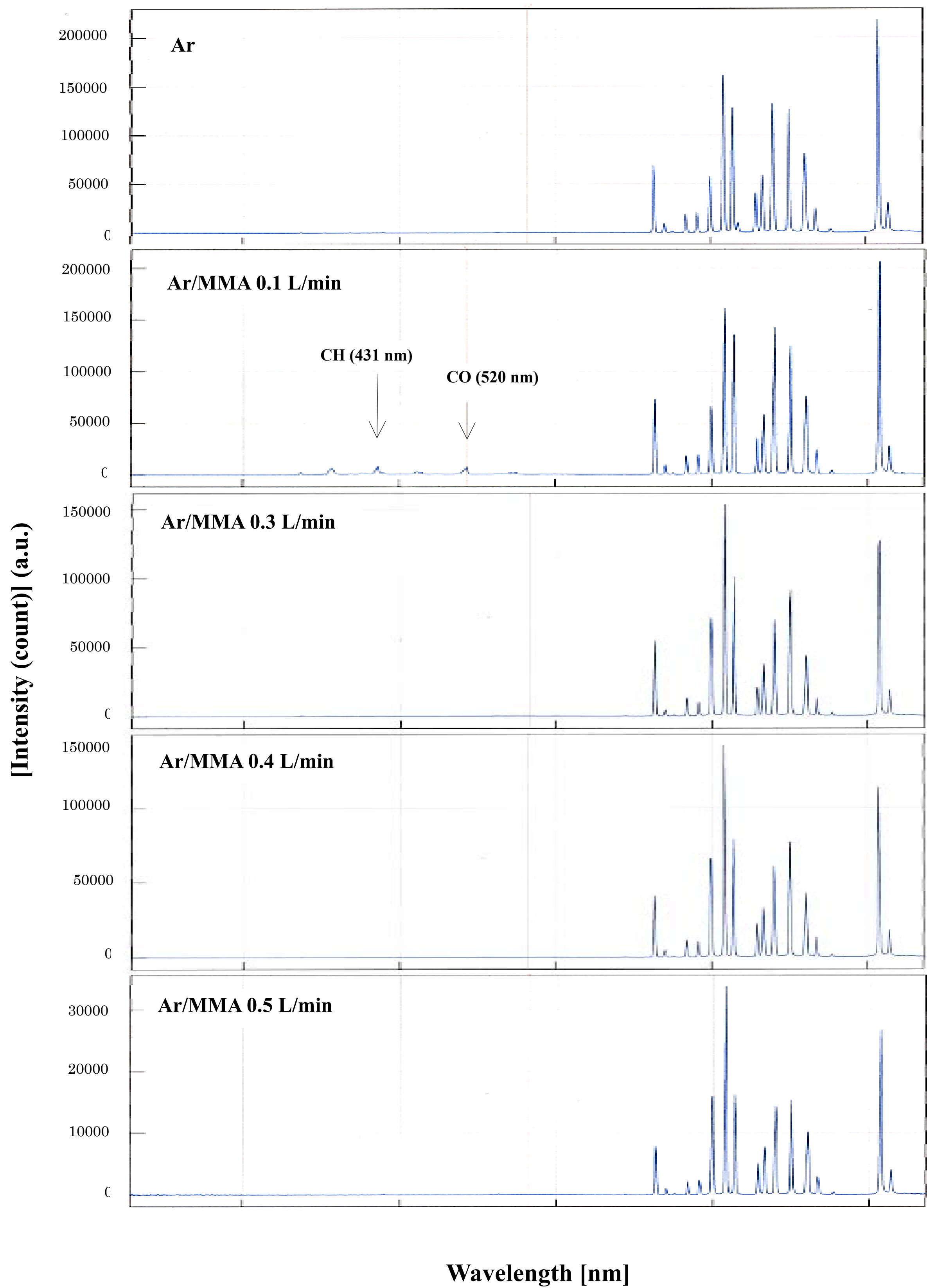

Figure 3.2. Emission lines of argon and Ar/MMA at different flow rates.

Conditions: Ar 3.0 L/min, applied voltage 4.0 kV, freq. 68.0 kHz.

excited species; however, it can be observed that the intensity of Ar lines has also decreased. This confirms that the plasma quenching phenomenon due to the energy efficient transfer from Ar metastables,[18] particularly the line at 912 nm (one can compare this line to the Ar line at 762 nm) to the MMA molecules. The quenching effect becomes more pronounced with increasing the monomer gas by feeding 0.5 L/min Ar since the emission intensity of Ar lines is decreased by the factor of 5. Further increase of monomer concentration by flowing more than 0.7 L/min extinguished the plasma. Considering that the emission from Ar* decreases when the monomer feeding rate increases from 0.1 to 0.3 L/min of Ar or even larger, the quenching reaction in plasma volume at rather high concentration of monomer indicates a low degree of monomer fragmentation. This is further supported by the fact that no lines of precursor fragments can be observed.

The OES results (showing no new lines of electronically excited species for the high concentration of the admixed monomer to Ar plasma) indicate that the fragmentation of MMA is negligible, and therefore that the monomer structure will be highly retained in the deposited films. The effect of carrier gas flow rate (concentration of monomer) on the quality of films was then investigated by FT-IR analysis.

FT-IR

Figure 3.3 shows the FT-IR spectra of several PPMMA films deposited using different flow rates of the carrier gas. Those spectra are displaced one in relation to another to avoid overlaps. It can be observed that, by flowing carrier gas with 0.1

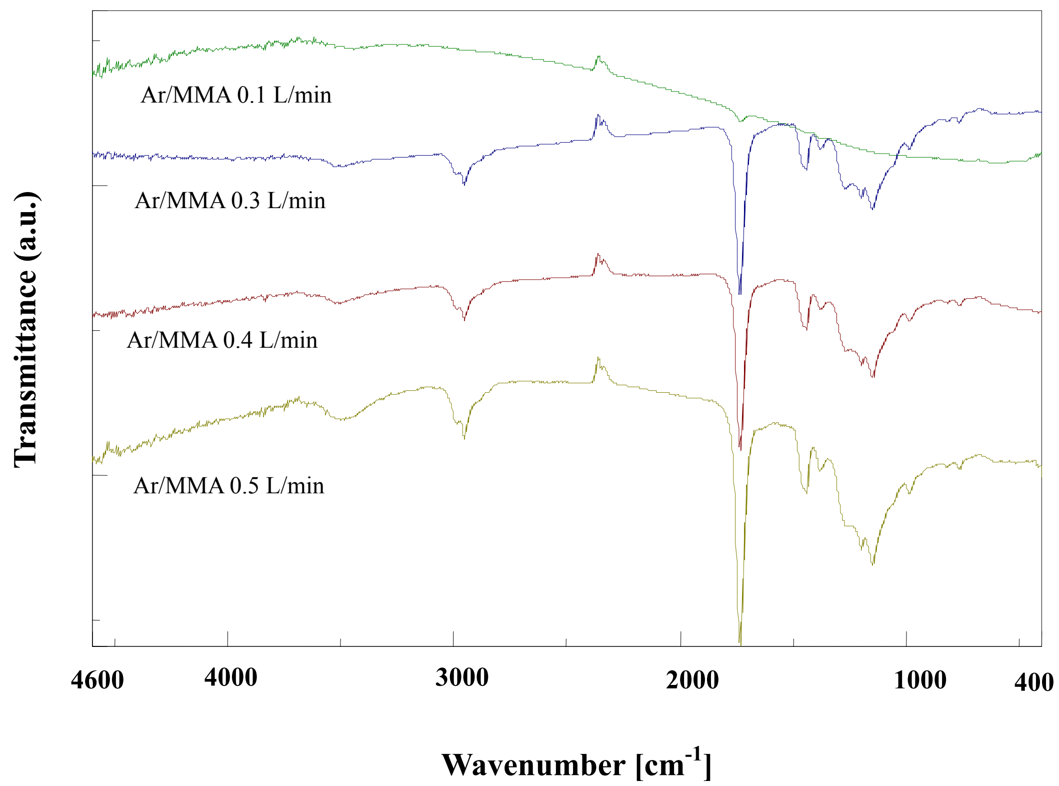

Figure 3.3 FT-IR spectra of PPMMA films deposited at different carrier gas flow rates.
Conditions: Ar 3.0 L/min, applied voltage 4.0 kV, frequency 68.0 kHz.

L/min, a weak band at around 1730 cm^{-1} which is due to the retention of C=O was obtained, while the other organic functional groups were not present. The vigorous fragmentation occurred in the plasma volume as mentioned above should be taken into account as one of the reasons of this phenomena. Moreover, the carbonyl double bonds seem to be reasonably stable during the reaction as identified by Christina M.Q. et al.[22] However, surprisingly, by enlarging Ar flow rate to 0.3 L/min, which corresponds to the point when the plasma turned out to the glow-like discharge, almost all characteristics of PMMA spectrum were retained in PPMMA film. Strong absorption bands at 1730 and 1460 cm^{-1} which correspond to the characteristic of C=O stretching of ester carbonyl and deformation of C–H bonds in the methyl group respectively are evident in the spectrum of PPMMA film. Moreover, two prominent peaks at 2990 and 2950 cm^{-1} attributed to the contribution of methyl and methylene groups and peaks in the region 1145-1270 cm^{-1} due to C–O–C stretching of the ester group are also remarkable. Because free radical polymerization is a typical reaction of plasma polymerization, it is suggested that the polymerization is primarily through the addition of vinyl radical to carbon-carbon double bond. This is supported by the absence of C=C absorption bands which usually present at around 1630 cm^{-1}. This is also in accordance with the findings of Ward et al.[23] when they deposited poly(acrylic acid) films by atmospheric pressure glow discharge using an ultrasonic nozzle. The extent of structural retention in the films deposited by monomer feeding of 0.3, 0.4 and 0.5 L/min Ar carrier gas seems to be the same, i.e. by comparing the intensity of C＝O relative to the intensity of C-H absorption bands. From FT-IR

results, it is interesting to mention that the well-defined chemical structure of our PPMMA films are resemble to that of conventional PMMA synthesized by chain polymerization. These films can be obtained directly from MMA monomer using an atmospheric pressure Ar plasma torch, when the characteristic discharge has transitioned from the filamentary to the glow-like regime.

Figure 3.4 represents the FT-IR spectra of several PPMMA films deposited using 3.0 L/min Ar, 0.5 L/min Ar/MMA and frequency 68.0 kHz, in respect to the differences of applied voltage. For a comparison, the spectrum of conventional PMMA film prepared by 2000 rpm spin coating (2 wt.-% of PMMA/acetone solution) is also shown. It can be seen that increasing the applied voltage did not give significant variations on the chemical structure of the deposited films. The extent of C＝O retention relative to the C-H retention of all the films deposited at difference applied voltage are comparable to that of the spin coated film. The difference in intensity could be attributed to the difference in film thickness, which was found to increase almost linearly from 215 nm obtained at 3.5 kV to 1080 nm obtained at 5.0 kV, through the measurements by using a surface profiler (ULVAC, Dektak 3ST). It can also be observed from Figure 3.4 that the inclusion of hydroxyl group around 3500 cm^{-1} is apparent, and it increases its intensity as a function of applied voltage. In order to clarify the factors of hydroxyl inclusion, the obtained films were kept in a desiccator before performing the FT-IR analysis. We found very little difference in spectra of the films kept in and outside of the desiccator, and this indicates that the inclusion of hydroxyl groups was mostly because of the incorporation of

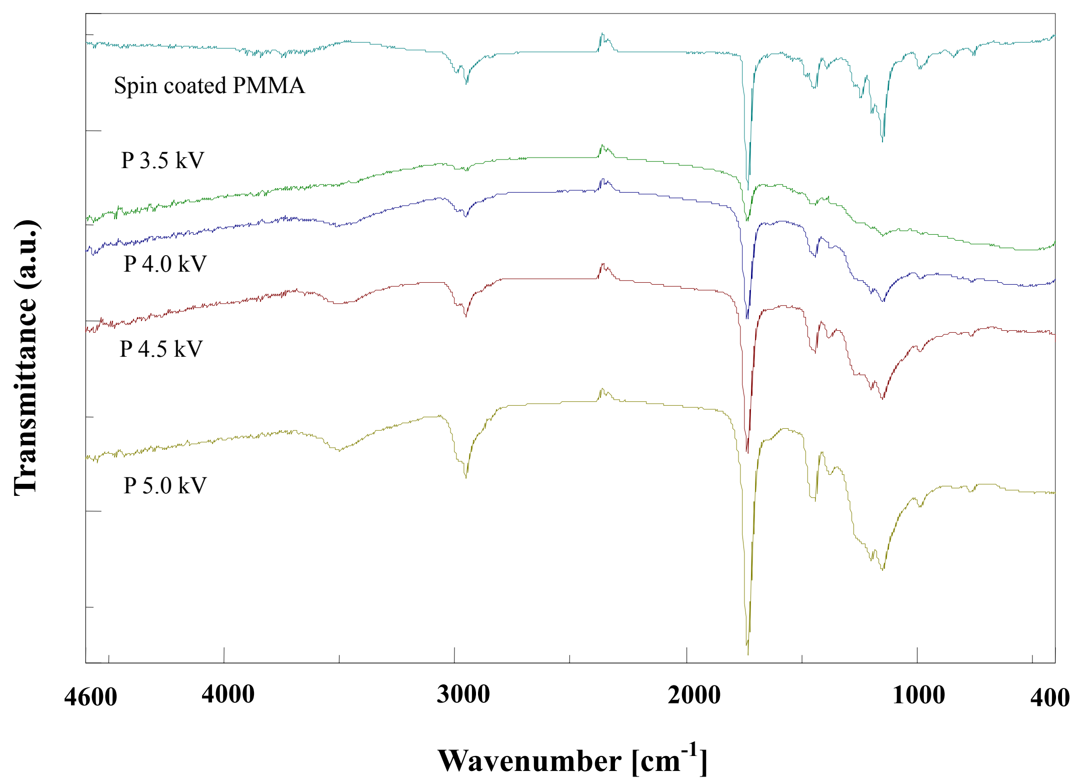

Figure 3.4 FT-IR spectra of PPMMA films deposited at different applied voltage. Conditions: Ar 3.0 L/min, Ar/MMA 0.5 L/min, frequency 68.0 kHz.

OH-containing fragments during the film growth rather than the water adsorption from the atmospheric air into the voids of the films. This hypothesis is also sustained by the observation that the OH concentration in our films increases with increasing the applied voltage (see the figure). The strong similarity in the structure of the PPMMA films with the conventional PMMA concluded by FT-IR analysis could become a confirmation that the non-equilibrium atmospheric pressure Ar plasma torch is one of the effective methods to produce organic thin films that resemble to the conventionally polymerized ones.

XPS

Figure 3.5 shows the typical high resolution C1s spectra of a spin coated conventional PMMA and a PPMMA film deposited at 4.0 kV with a flow rate of 0.3 L/min Ar/MMA, respectively. Those spectra have been curve-fitted to discern characteristic of bonding components at different binding energies. The curve-fitted C1s spectrum of conventional PMMA presents three peaks at 285.2 eV, 286.7 eV and 289.0 eV, which are attributed to the C−C/C−H bonds, C−O bonds and O−C=O functional groups, respectively. The C1s scan of PPMMA film shows the same characteristic bonding to PMMA at the similar binding energies with an additional peak at 287.8 eV that corresponds to the C=O or O−C−O moieties. This peak could be possibly occurred due to the loss of an ester carbon through the scission of the ester methoxy.[24] Table 3.1 summarizes the relative abundant percentages of each functional group estimated from the deconvolution of C1s spectra for the two films.

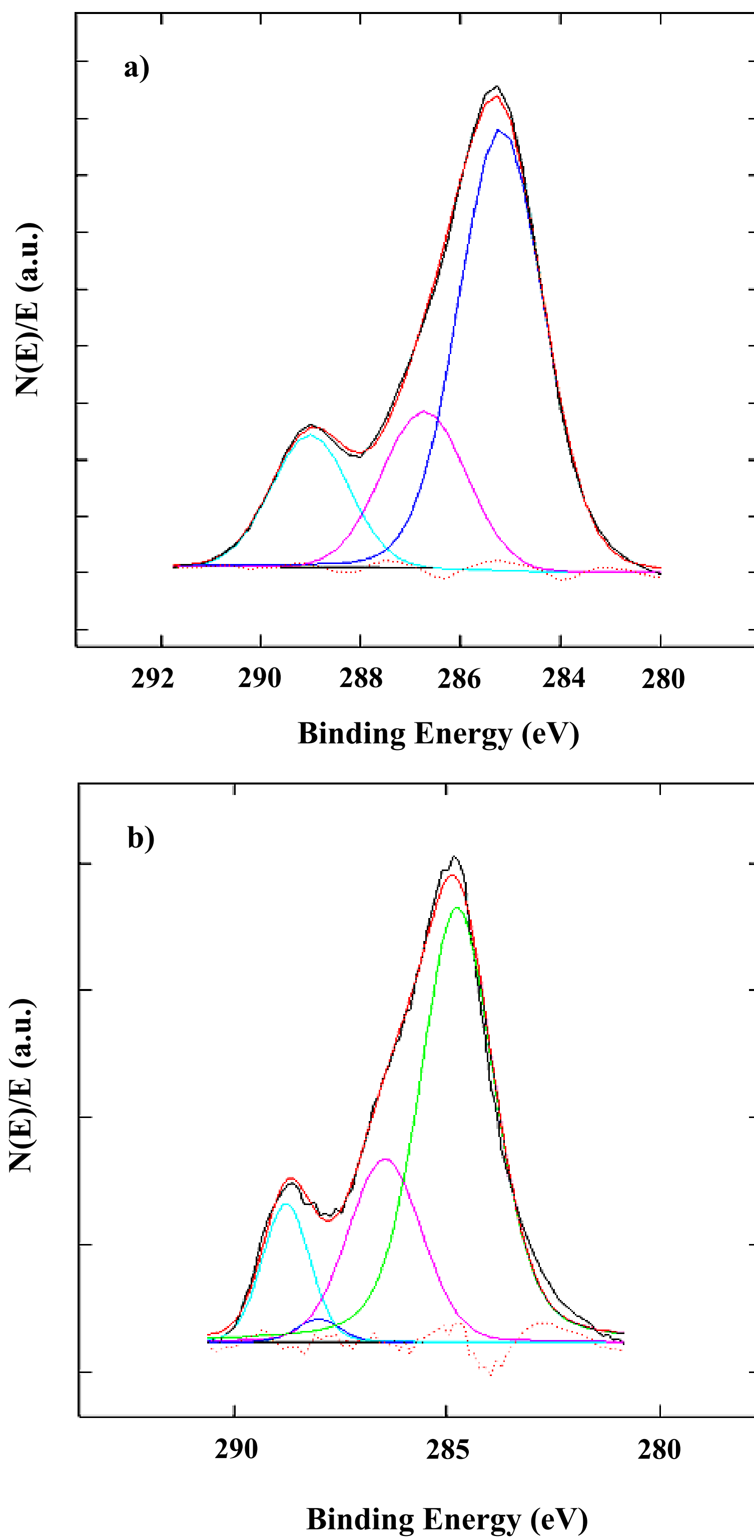

Figure 3.5. C1s high resolution of a) PMMA spin coated film and b) PPMMA film deposited at 4.0 kV, 68.0 kHz and Ar/MMA 0.3 L/min.

Table 3.1. Chemical composition and relative abundance of each functional group in high resolution C1s of films.

Films	Relative Abundance of Each Functional Group (%)			
	C−C / C−H	C−O	C=O / O−C−O	O−C=O
Spin coated PMMA	62.7	21.0	0	16.3
PPMMA	65.6	20.7	2.3	11.4

Compared to the conventional PMMA film, the relative abundance values of each functional group in PPMMA film are close, with the exception of the retention of O－C＝O groups. Lower percentage of this group in PPMMA relative to the PMMA indicates the loss of ester functionalities, which might be responsible for the formation of the new functional group of C＝O or O－C－O that was absent in PMMA. In general, good comparable features of PMMA and PPMMA film analyzed by XPS study can make a confirmation that even the uppermost surface of PPMMA film deposited by the non equilibrium atmospheric pressure plasma torch has similar characteristic feature with conventional PMMA surface.

From a practical point of view, the sensitivity of the deposition toward oxygen traces is an important issue. The experiments in which the addition of oxygen was therefore conducted in order to know the influence of the possible oxidation reaction in the reactor to the structure of deposited film. The addition of 50 mL/min oxygen flow into reactor was found not to affect the chemical structure of film, leading to implication that this process might be utilized in open air (in case to deposit the complex shape) with the same achievement by using a reactor.

Conclusion

A non-equilibrium atmospheric pressure plasma torch that can sustain Ar plasma has

been developed and successfully demonstrated the ability to be used to obtain organic thin films through the plasma polymerization of MMA. OES study showed a low degree of fragmentation in plasma phase when the admixed MMA was flowed by a flux of 0.3 L/min Ar carrier gas. These conditions can therefore lead to a high degree of monomer retention in the film structure. FT-IR and XPS analyses confirm that PPMMA films have similar chemical structure and composition to those of the conventional polymer. Finally, the present paper reveals that the non-equilibrium atmospheric pressure plasma torch using Ar as the working gas can become one of the effective methods to deposit organic thin films with characteristics similar to the corresponding conventional polymers.

References

1. A. Hiratsuka and I. Karube, *Electroanalysis*, **12**, 695-702 (2000).
2. S. Morita, J. Tamano, S. Hattori and M. Ieda, *Journal of Applied Physics*, **51**, 3938-3941 (1980).
3. C. Zhang, J. Wyatt, D.H. Weinkauf, *Polymer*, **45**, 7665-7671 (2004).
4. A.R.K. Ralston, J.A. Tobin, S.S. Bajikar, D.D. Denton, *Sensors and Actuators B*, **22**, 139 (1994).
5. H.S. Jeon, J. Wyatt, D. Harper-Nixon, D.H. Weinkauf, *J. of Polym. Sci.*, *Part B: Polym. Physics*, **42**, 2522-2530 (2004).
6. T. Yokoyama, M. Kogoma, S. Kanazawa, T. Moriwaki and S. Okazaki, *J. Phys. D: Appl. Phys.*, **23**, 374-377 (1990).
7. Y. Sawada, S. Ogawa and M. Kogoma, *J. Phys D: Appl. Phys.*, **28**, 1661-1669 (1995).
8. R. Prat, Y.J. Koh, Y. Bubukutty, M. Kogoma, S. Okazaki, M. Kodama, *Polymer*, **41**, 7355-7360 (2000).

9. C.P. Klages, K. Hopfner, N. Klake and R. Thyen, *Plasmas and Polymers*, **5**, 79-89 (2000).

10. A. Sonnenfeld, T.M. Tun, L. Zajícková, K.V. Kozlov, H.E. Wagner, J.F. Behnke and R. Hippler, *Plasmas and Polymers*, **6**, 237-266 (2001).

11. R. Foest, F. Adler, F. Sigeneger, M. Schmidt, *Surf. Coat. Technol.*, **163-164**, 323-330 (2003).

12. S.E Babayan, J.Y. Jeong, V.J. Tu, J. Park, G.S. Selwyn and R.F. Hicks, *Plasma Sources Sci. Technol.*, **7**, 286-288 (1998).

13. S.E Babayan, J.Y. Jeong, A. Schutze, V.J. Tu, M. Moravej, G.S. Selwyn and R.F. Hicks, *Plasma Sources Sci. Technol.*, **10**, 573-578 (2001).

14. G.R. Nowling, S.E. Babayan, V. Jankovic and R.F. Hicks, *Plasmas Sources Sci. Technol.*, **11**, 97-103 (2002).

15. Y. Mori, K. Yoshii, H. Kakiuchi and K. Yasutake, *Rev. Sci. Instrum.*, **71**, 3173 (2000).

16. H. Kakiuchi, Y. Nakahama, H. Ohmi, K. Yasutake, K. Yoshii and Y. Mori, *Thin Solid Films*, **479**, 17-23 (2005).

17. S. Wang, V. Schulz-von der Gathen, and H.F. Dobele, *Applied Physics Letters*, **83**, 3272-3274 (2003).

18. K. Wagatsuma, *Spectrochimica Acta Part B: Atomic Spectroscopy*, **56**, 465 (2001).

19. S.E. Alexandrov, N. McSporran, M.L. Hitchman, *Chem. Vap. Deposition*, **11**, 481 (2005).

20. A. Bogaerts, R. Gijbels, J. Vlcek, *Spectrochimica Acta Part B*, **53**, 1517 (1998).

21. R.W.B. Pearse, A.G. Gaydon, *The Identification of Molecular Spectra*, Fourth Edition, Chapman and Hall, (1976).

22.Christina M.Q., G.G.B. de Souza and J.B. Maciel., *J. Braz. Chem. Soc.*, **9**, 521 (1998).

23. L.J. Ward, W.C.E. Schofield, J.P.S. Badyal, *Chem. Mater.*, **15**, 1466 (2003).

24. T.B. Casserly and K.K. Gleason, *Chem. Vap. Deposition*, **12**, 59 (2006).

CHAPTER IV

Non-equilibrium Atmospheric Pressure Argon Plasma Torch For Deposition of Thin Silicon Oxide Film

Abstract

A non-equilibrium atmospheric pressure plasma torch that can be generated either in He or Ar gas by using pulsed high voltage power supply with the discharge temperature in the range of 22-35℃ has been developed. This system has been used to deposit silicon dioxide film from hexamethyldisiloxane (HMDSO) precursor diluted in oxygen carrier gas. It was concluded that Ar plasma was more powerful than He plasma for depositing SiO_2-like film in terms of both quality and deposition rates at the same applied power, frequency and gas composition. The feed rate of HMDSO/O_2 injected to the Ar plasma torch was limited up to 100 mL/min to ensure inorganic coatings were deposited. In order to improve the quality of the visual aspect without deteriorating the inorganic feature of the film, a small amount of nitrogen (N_2) gas has been admixed to the Ar gas as the working gas. When the composition ratio of Ar and N_2 flow gas was 30:1, the regime behavior was transformed from filamentary

into glow-like discharge owing to the quenching effect of the N_2 gas on Ar plasma. These conditions can therefore result in better property of the film with no appearance of the small particles on the film surface.

Introduction

As reported in the previous chapter, the non-equilibrium atmospheric pressure Ar plasma torch can be used to deposit film from organic monomer (methyl methacrylate) which has similar characteristics to the PMMA film obtained conventionally. This chapter will report the study of deposition of SiO_2-like film from monomer having an inorganic feature (hexamethyldisiloxane, HMDSO) using an atmospheric pressure Ar plasma torch as well. SiO_2-like films are greatly of interest because of having excellent physical and chemical properties such as optical transparency, chemical inertness, scratch resistant and sufficient hardness, thus are widely used in many fields of technological applications. Microelectronics, optic, biomedical, metal and polymer protection coatings and food packaging are the fields that find the utilization of silicon oxide film in their industry applications.

At present, the well-established method which is commonly utilized for the deposition of organic or inorganic films is low pressure plasma-assisted processes. However, the necessity of an expensive vacuum system is the biggest shortcoming of this process in the industrial applications, besides the limitation to the batch system processes. Therefore, to overcome those disadvantages, considerable efforts are crucial in developing the alternative techniques. The non-equilibrium atmospheric pressure plasma is one of the most promising methods to deposit polymer films in the more flexible, reliable, less expensive and continuous way of treatment. Several types

of non-equilibrium atmospheric pressure plasma sources have been successfully used for depositing SiO_2 films to substrate surface such as atmospheric pressure (AP) dielectric barrier discharge (DBD)[1-4] as the most commonly used atmospheric pressure discharge, AP Plasma Jet, [5,6] and AP plasma chemical vapor deposition (AP-PCVD).[7,8] However, most of them have used helium (He) as the working gas to generate the plasma. If the plasma can be generated with using argon (Ar) as the working gas, it will bring a great benefit to the technique as Ar gas is much less expensive than He gas. Moreover, Ar plasmas shows better energy transfer efficiency than the He plasmas under the same working conditions.[9] We have successfully developed a non-equilibrium atmospheric pressure plasma torch in which the plasma can be generated either in He or in Ar gas. This system has been used to deposit an organic film (PPMMA) and exhibits similar chemical characteristics to the spin coated conventional PMMA film.[10]

The present research reports the deposition of SiO_2-like films by means of a non-equilibrium atmospheric pressure Ar plasma torch using HMDSO as the precursor diluted in oxygen. The film deposited using He plasma at the same condition is also shown for the comparison. The properties of deposited films have been characterized by FT-IR, XPS and SEM as well as laser microscope.

Experimental

The schematic diagram for the atmospheric pressure plasma polymerization is shown in Figure 4.1. High voltage power supply (Haiden Lab PHF-2K) was

connected to the stainless pipe ($\phi_{in.}$ = 4 mm) electrode which was embedded in the middle of a perforated silicon stopper and allowing the working gas to flow through. The stainless tape electrode that circled the outer part of the stopper was connected to

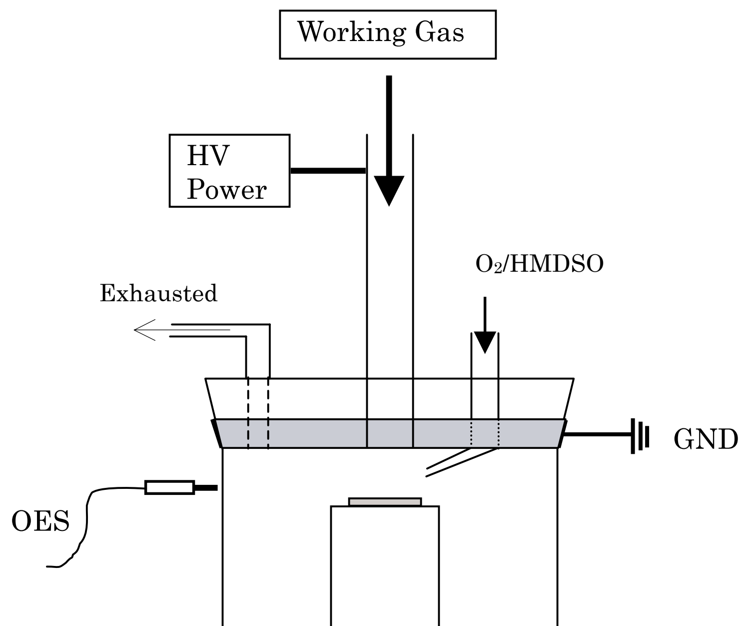

Figure 4.1. Schematic diagram of non-equilibrium atmospheric pressure Ar plasma torch for deposition of SiO_2-like films.

the ground. 3.0 L/min of working gas (He or Ar) was allowed to flow through the pipe and the plasma was generated at the frequency of 68.0 kHz downstream to the substrate which was positioned along 2.5 cm distance from the stainless pipe electrode.

HMDSO monomer that was stored in room temperature was diluted in the oxygen carrier gas. Its vapor was introduced separately into the middle of the plasma jet downstream to the substrate surface at a different oxygen flow rate. Polymer films were deposited on KBr disk for FT-IR analysis and silicon wafer for the other measurements. All of deposition processes were carried out for 10 minutes without substrate heating.

Optical emission spectroscopy (OES) measurements were performed perpendicularly to the plasma jet with a Multiband Plasma-Process Monitor (MPM, Hamamatsu Photonics C7460). The emission spectra from the plasma source were acquired through the equipped optical fiber in the range of 200-950 nm. FT-IR analyses were performed to examine the chemical structure of SiO_2-like films. Transmission mode was used for FT-IR measurement on a Jasco FT-IR-8000 spectrophotometer with 64 scans at 4 cm^{-1} resolution. XPS measurements were carried out by a Perkin Elmer PHI Model 5600 ESCA instrument, using a monochromated Al X-ray source. The binding energy scale was calibrated by setting the C1s peak at 285 eV. Carbon (C1s), oxygen (O1s) and silicon (Si2p) atomic

compositions were also evaluated. The surface morphologies of the films were observed by both a scanning microscope electron (SEM; Hitachi S5000) and a laser microscope (Keyence VK-9500).

Results and Discussion

Effect of Working Gas

Figure 4.2 shows the FT-IR spectrum of HMDSO monomer and plasma polymerized HMDSO films deposited by means of a non-equilibrium atmospheric pressure plasma torch using He and Ar as the working gas, in which all the other parameters were kept constant. The spectrum of HMDSO monomer (Fig. 4.2.a) exhibits the absorbance bands of C–H stretching in Si–CH_3 at 2965 cm^{-1}, Si–CH_3 bending at 1260 cm^{-1}, cm^{-1}, Si–O–Si stretching at 1020 cm^{-1} and Si–CH_3 rocking vibration at 850 cm^{-1}.[11,12]

When the He working gas was used for the deposition, the chemical structure of the film (Fig. 4.2.b.) retained almost all characteristics of the monomer. In addition, new absorption bands which were absent in the monomer spectrum are recognized in the spectrum of plasma polymerized SiO_2-like film, i.e. Si–OH band at 930 cm^{-1} and the broadband around 3400 cm^{-1} and also another Si–O–Si network around 450 cm^{-1}. However, when the deposition was carried out by using Ar plasma jet while keeping all other parameters the same, the chemical structure of the film had been changed significantly, i.e. no –CH_3 absorption band was detected which resulting in an inorganic film (Fig. 4.2.c). This SiO_2-like film deposited using Ar plasma without substrate heating seemed indistinguishable from the SiO_2 film obtained by Babayan et.al.,[6] which was deposited by atmospheric pressure plasma He jet using

tetraethoxysilane with heating the substrate to 115℃. Additionally, as can be seen from the figure, the difference of the band intensities in both of SiO_2-like films spectra indicates that the deposition carrying by Ar plasma has a higher growth rate than that

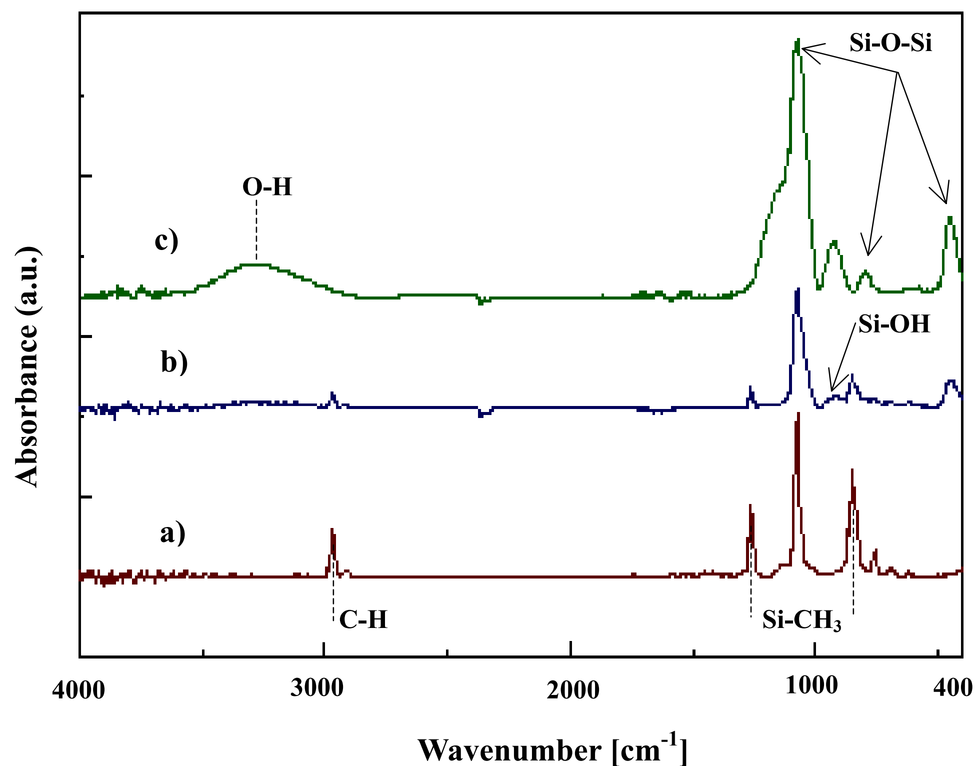

Figure 4.2. FTIR spectrum of a) HMDSO monomer and the corresponding of the deposited films using b) He plasma torch and c) Ar plasma torch. Conditions: flow gas 3.0 L/min, applied voltage 3.5 kV, f 68.0 kHz and O_2/HMDSO 50 mL/min.

by He plasma. In order to confirm this suggestion, the absorbance of Si–O–Si bond at 1070 cm^{-1} of the films deposited in He and Ar plasmas was plotted against the deposition time through FT-IR measurements, and the results are shown in Figure 4.3. The plot exhibits that the absorbance of the characteristic band of films deposited by He and Ar plasma have similar tendency, i.e. increases with deposition time. However, the magnitude is larger for the sample prepared under Ar plasma than sample prepared under He plasma. As it is known that the absorbance is proportional to the thickness of the sample, thus the growth rate (thickness per unit time) of the film deposition is faster in Ar than that in He. The difference in working gas to generate the atmospheric pressure plasma leads to a conclusion that Ar plasma can deposit SiO_2-like film more efficiently than the He plasma in terms of film composition and deposition rate.

It is very important to understand the reasons of why the termination mentioned above could have occurred. Wang et al.[9] found that the temperature at the exit of the nozzle of Ar/O_2 RF plasma jet is about 100 K higher than that for the He/O_2 plasma jet under the same conditions of the input power, the flow rate and composition of gas, which tells that the efficiently of gas heating is much better in the former plasma. However, the gas temperature of our plasma jet showed almost similar values in the range of 22-35℃ (the increment as a function of the processing time) for both of He and Ar plasmas as discussed in Chapter II. We therefore examine the

optical emission spectroscopy to interpret the question.

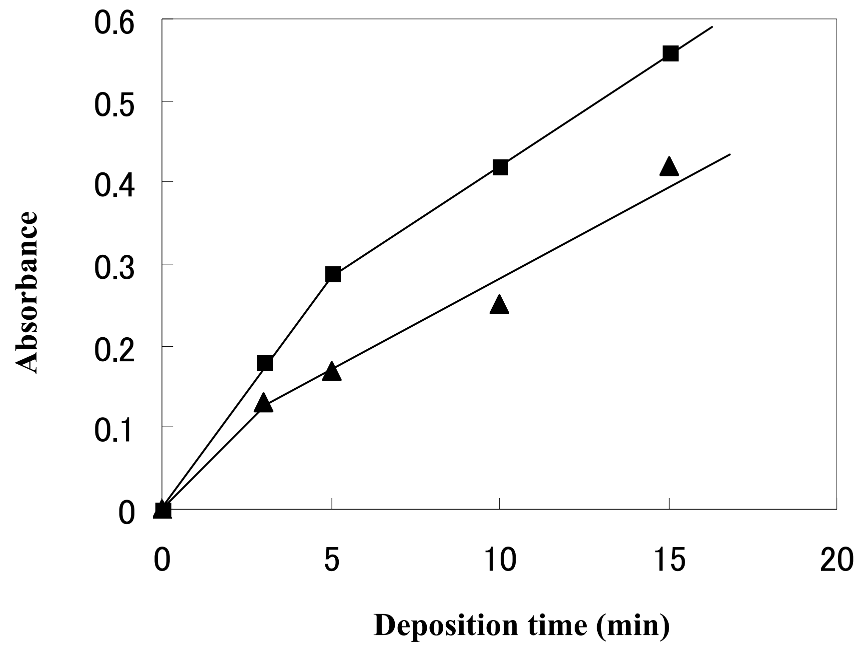

Figure 4.3. Absorbance of Si–O–Si bond at 1070 cm^{-1} of the films deposited in He (▲) and Ar (■) plasma plotted against deposition time.

Optical Emission Spectroscopy (OES)

OES has been performed to get some insight of deposition process of SiO_2-like films from the chemistry of plasma-phase. Shown in Figure 4.4 are the typical emission spectra of He and Ar plasma jet recorded in the wavelength range from 200 to 900 nm. The emission spectrum of He plasma contains spectral bands of He species with the most intense line at 706.5 nm ($3^3S \longrightarrow 2^3P$).[13,14] The spectrum also includes a group of N_2 emission in the form of first negative system and second positive system, as well as the population of atomic oxygen at 777.4 nm and 844.6 nm. These signal bands are the consequence of N_2 and O_2 impurities in the reactor which are readily ionized and excited through the energy transfer of Penning collisions.[15,16] When the plasma is generated, it should be noted that the discharge is mainly based on helium, as the emission intensity of He is dominant in the spectrum. In contrast to He, the spectum of Ar plasma shows highly intense electronically excited Ar neutrals lines lying around 700-900 nm without the presence of any additional lines of impurity. This might be due to the fact that the energy of Ar metastables (11.5 eV) or the excitation threshold (13.5 eV) are not energetically sufficient enough either to excite the first negative system of nitrogen at 391.4 nm which needs 18.7 eV[17], or to emit the atomic oxygen atom at 777.4 nm that requires at least 16 eV through a single-step dissociative excitation.[18] These lines are quite similar to the spectral Ar lines either from an atmospheric pressure barrier discharge[19] or that from hollow cathode

discharge under 1 torr.[20]

Despite the information of active species recorded at particular wavelengths from He and Ar plasma, one can see that the relative emission intensities of the lines

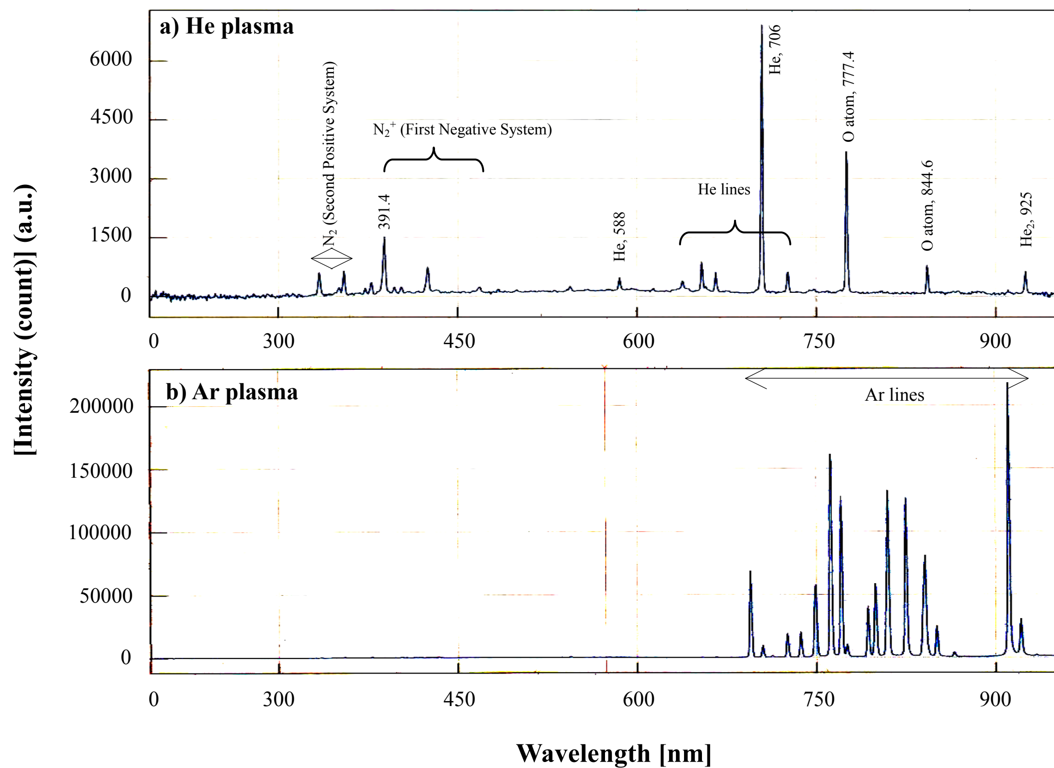

Figure 4.4. Typical optical emission spectrum of a) He and b) Ar plasma torch. Discharge parameters: gas flow 3.0 L/min, applied voltage 3.5 kV and frequency 68.0 kHz.

from those plasma are very different from each other, which will affect the behavior of the high-energy tail of the electron energy distribution functions (EEDF). By taking into account that the emission intensities of He and Ar plasma can be related to the density of electrons with energy higher than their excitation thresholds, 23.0 eV and 13.5 eV respectively,[21,22] it could be deduced that comparing to the He plasma, the shape of EEDF curve of Ar plasma shifts to the higher energy level, on account that the population of high energy electrons increases more rapidly than that of the low energy ones. This means that even though the electron energy of Ar plasma is lower than that of He plasma, its density is much larger than He plasma. As a result, when oxygen and precursor are injected to the Ar plasma, much population of oxygen and silicon containing active species contributing to the film formation are produced more than in He plasma. Taking it additionally into account that almost all covalent bond in HMDSO and diatomic oxygen could be dissociated by Ar plasma, it is reasonably understood that Ar plasma can deposit more rapidly the films with more inorganic characteristics than by using He plasma as shown in FT-IR study.

Figure 4.5 exhibits the emission spectra of He and Ar plasma jet with injection of HMDSO precursor diluted in O_2 carrier gas. It is shown that the concentration of all active species in He and Ar plasmas are depopulated with the precursor admixture to the plasma. In addition, the reaction involving high energy electrons leads to the emission of new species which were absent in the pure He and Ar plasma. As shown

in Figure 4.5.a, the highest intensity is recorded at 777.4 nm attributed to O atom, which supports the above explanation that as the content of O_2 increases by injection to the He plasma, the He threshold energy is consumed and lead to the dissociative

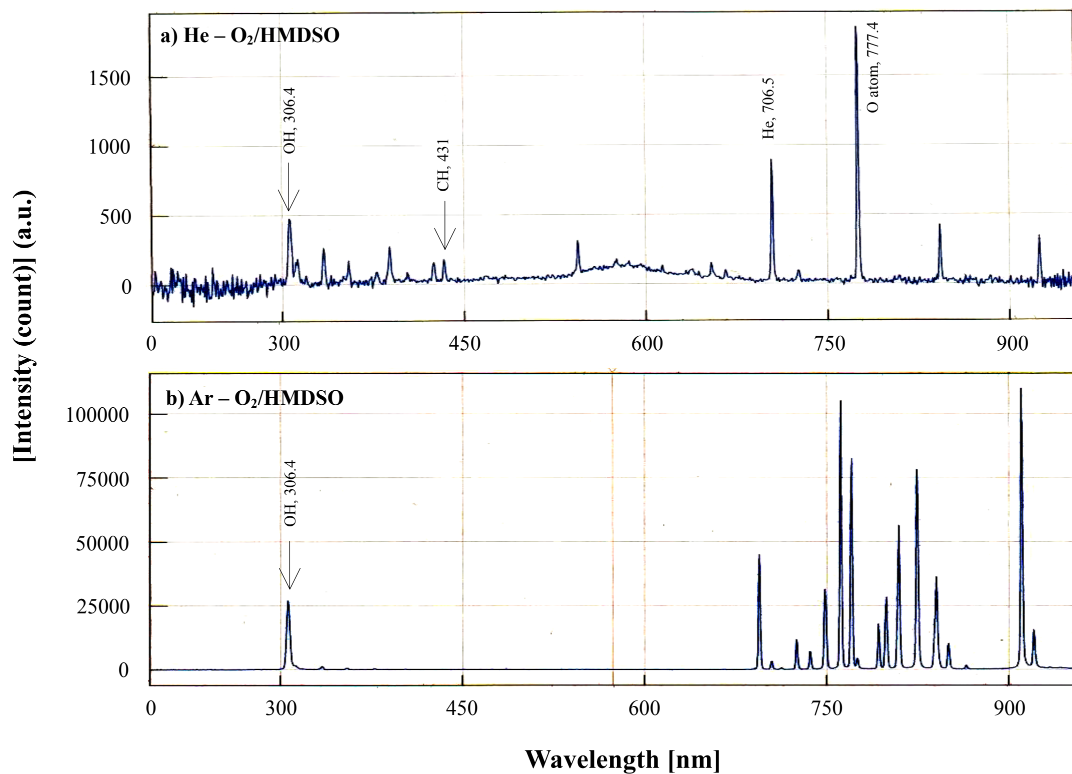

Figure 4.5. Emission spectrum of a) He-O_2/HMDSO and b) Ar-O_2/HMDSO plasma torch. Discharge parameters: gas flow 3.0 L/min, applied voltage 3.5 kV, frequency 68.0 kHz and O_2/HMDSO 50 mL/min.

excitation of oxygen. Other product of precursor dissociation through the similar reaction is CH line at 431 nm recognized only in He–O_2/HMDSO plasma (Fig. 4.5.a), which can reflect the incorporation of carbon containing group on the deposit film. Moreover, OH emission at 306.1 nm is clearly observed and this species shows more intensely in Ar-O_2-HMDSO plasma (Fig 4.5.b). The identification of OH in both plasmas confirms the inclusion of silanol group occurs during the film growth more likely than by the oxidation reaction post deposition.

Effect of Carrier Gas Flow Rate

The effect of O_2 carrier gas flow rate on the chemical structure of the films analyzed by FT-IR spectra is shown in Figure 4.6. These experiments were using 3.0 L/min flow of Ar gas to generate the plasma torch. The flow rates of oxygen through the bubbler of HMDSO vessel at constant temperature were between 30 to 300 ml/min resulting in increasing concentration of HMDSO from 555 to 5048 ppm. It can be seen that by using O_2 flow rate from 30 mL/min to 100 mL/min to vaporize the precursor introduced to Ar plasma, the films obtained have inorganic characteristic as exhibited by no detection of hydrocarbon group in the spectra. However, increasing the O_2 flow rate to 200 and 300 mL/min leads to the growing organic moieties to the chemical structure of films. Besides the existence of –CH_3 groups at 2965 cm^{-1} and 1260 cm^{-1}, one also can observe the evolution of another –CH_3 around 850 cm^{-1} which

is a shoulder at 200 mL/min O_2 flow rate, and becomes a clearly peak using 300 mL/min O_2 feed. The growing organic content in the films may probably also cause changes in the shape of Si–O–Si band around 1040 cm^{-1} to a broader peak and shifts

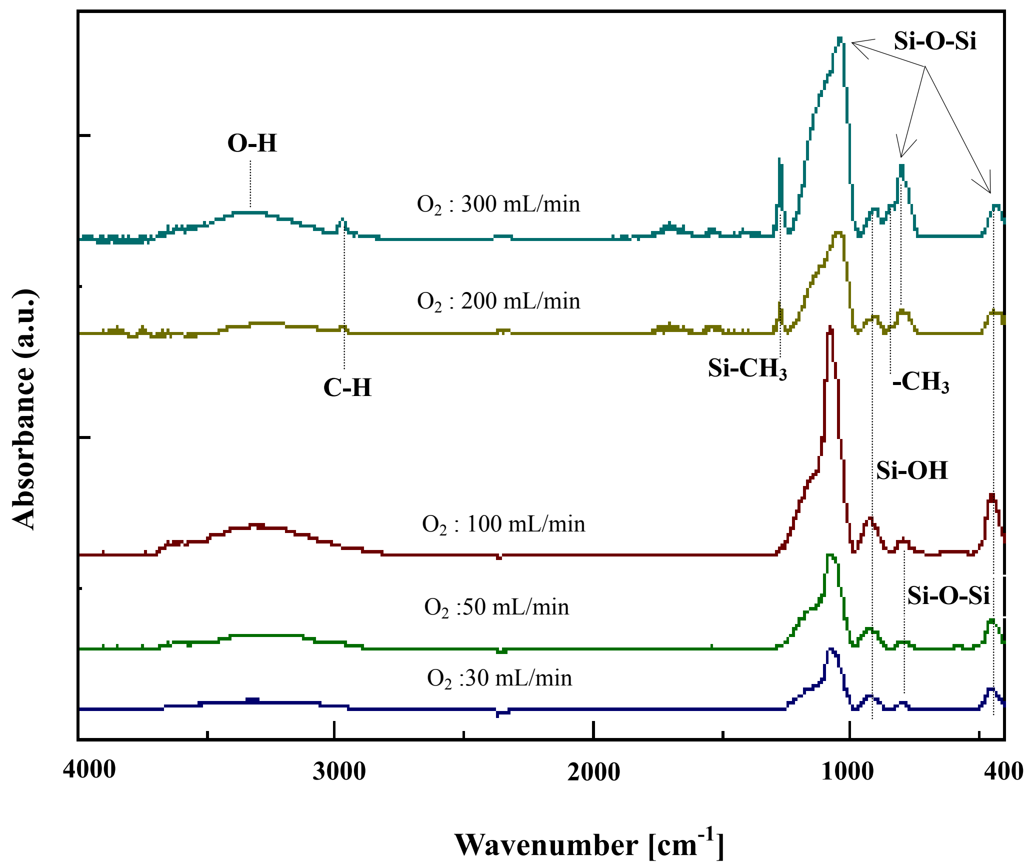

Figure 4.6 FT-IR spectrum of PPHMDSO films deposited at difference of O_2 carrier gas. Discharge parameters: Ar 3.0 L/min, applied voltage 4.0 kV and freq. 68.0 kHz, O_2/HMDSO 50 mL/min.

the peak to lower wavenumbers.[23] It is acceptable to understand that the electric energy consumed for the activation of precursor will be gradually insufficient by increasing precursor concentration. In our plasma torch system the concentration of HMDSO allowable for making a complete chemical transformation from HMDSO to SiO_2 should be when the flow rate of oxygen carrier gas was lower than 100 mL/min under the applied voltage of 4.0 kV.

XPS Study

The chemical composition of the films was also investigated by XPS analysis. The calculated percentages of silicon, carbon and oxygen, as a function of O_2 carrier gas flow rate are shown in Figure 4.7. Even the carbon containing moieties were not detected in FT-IR analysis, the concentration of the atomic carbon on the top surface of the films still could be identified by XPS. A quite low concentration of carbon (less than 6 %) is present on the films deposited by feeding the O_2 carrier gas up to 100 mL/min. As shown in the figure, increasing O_2 flow rate leads to a significant increase of carbon content and a substantial decrease of oxygen component, while the percentage of silicon varies a little, that is from 28.8 % to 26.0 %. These results from XPS study confirm the results from FT-IR study that the increase of carbon content of the film, which is identical to the growing of organic moieties in the film formation, arises when the HMDSO was injected by feeding the oxygen with the flow rate higher

than 100 mL/min.

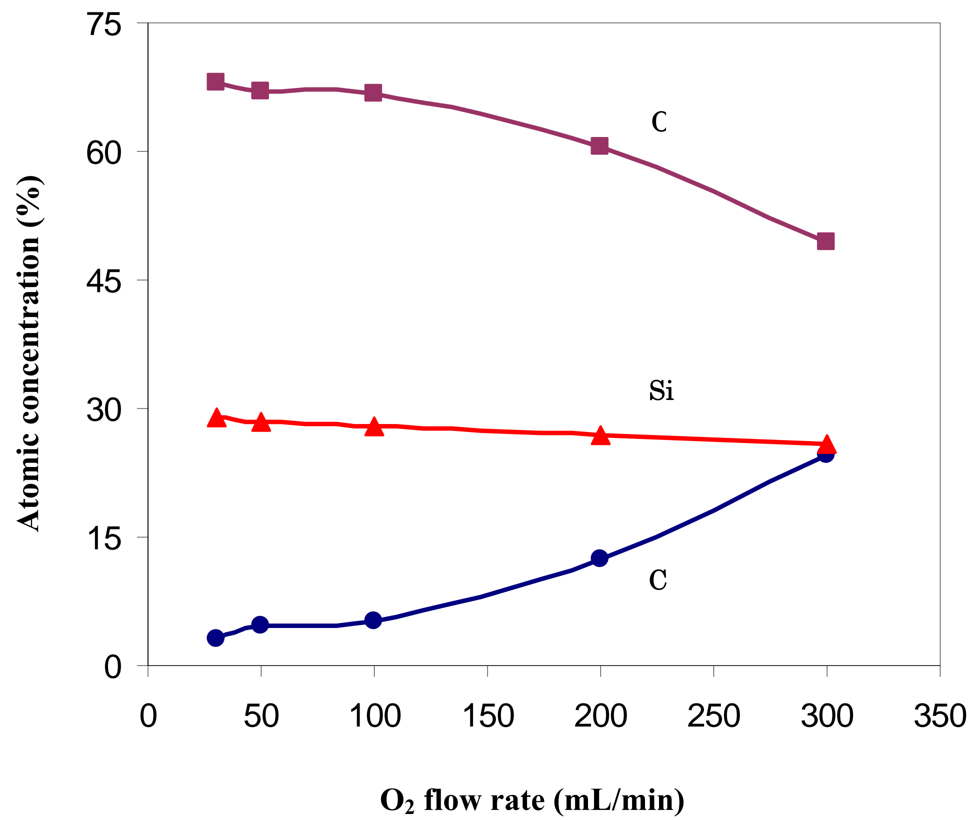

Figure 4.7. Relationship of surface atomic percentages of C, O and Si in the film as a function of O_2 carrier gas flow rates.

Improvement of Visual Aspect of Deposited Films

All of deposit films obtained using Ar plasma with O_2-HMDSO mixtures were found to yield powder formation on their surface. The observation of the sample using scanning electron microscope depicted in Figure 4.8 shows the unexpected powder contamination on the film surface. The powderous materials which were probably formed due to the gas phase nucleation[22] are the possible results of reaction between the monomer containing inorganic material and the filamentary Ar discharge in the presence of oxygen.

A lot of experiments have been performed in order to improve the quality of the films. One of the thoughts is how to generate a glow discharge based on Ar gas, instead of the filamentary one, to assist the process of deposition. We finally examine the experiments by using the combination of Ar and N_2 to generate the plasma. The nature of filamentary discharge of Ar plasma has been reduced remarkably when a small amount of N_2 was admixed to Ar as a source gas. This is reasonable since the N_2 has a function to give a quenching effect to the Ar plasma. Investigation of the discharge behavior based on mixed Ar and N_2 revealed that the best combination of Ar and N_2 should be 30:1 in flow rate ratio to give rise a glow-like discharge, in the sense that the light intensity appeared to be homogenous, which resembled to the glow discharge generated by He gas. Therefore, this glow-like discharge with a mixture of Ar and N_2 as the working gas was utilized to deposit HMDSO film onto substrate with

the same schematic arrangement as before.

FT-IR spectrum of the film can be seen in Figure 4.9. The film has been deposited by using a mixture gas of 3.0 L/min Ar and 0.1 L/min N_2 at applied voltage

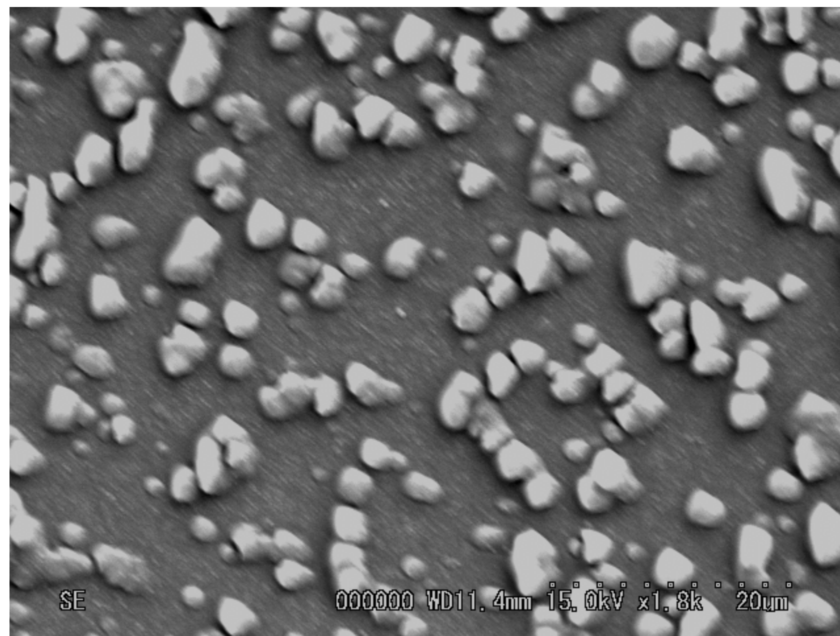

Figure 4.8. A SEM image of film surface deposited using pure Ar plasma and O_2/HMDSO admixture.

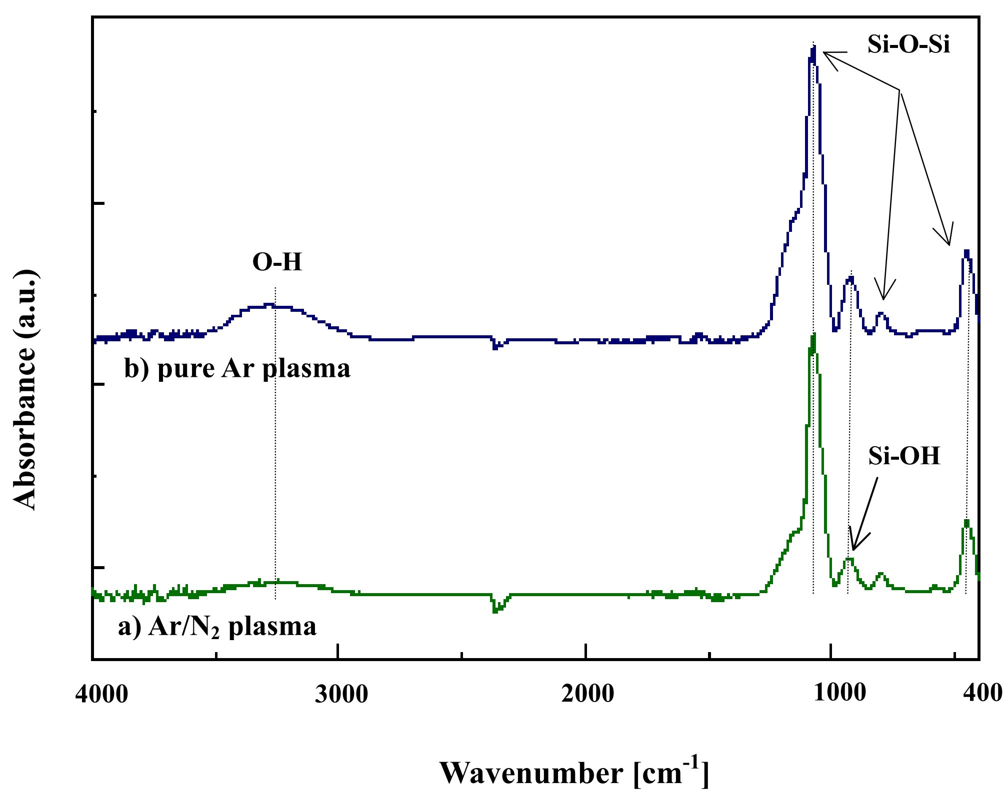

Figure 4.9. FT-IR spectrum of SiO_2-like film deposited using glow-like Ar-N_2 discharge (a) and the comparison of film deposited using Ar as the working gas (b). Conditions: Ar 3.0 L/min, N_2 0.1 L/min, applied voltage 4.0 kV and freq 68.0 kHz, O_2-HMDSO 50 mL/min.

4.0 kV, frequency 68.0 kHz and 50 mL/min O_2-HMDSO. It is observed that the chemical structure of the film deposited using Ar/N_2 plasma shows no remarkable difference from that of the film deposited using pure Ar plasma at same conditions, particularly no organic residue is detected. Moreover, the spectrum also does not show any absorption band of nitrogen-containing functional groups. The quality of the film even exhibits better property since the silanol groups has a smaller intensity, which will lead to a better chemical stability of the coatings.

The visual aspect of the film deposited using Ar/N_2 plasma also shows better property than the film deposited by Ar plasma since the powderous region is not observed on the surface of the film. The dense transparent film obtained by Ar/N_2 plasma with the thickness of 300 nm through the measurements by using a laser microscope (Keyence VK-9500) seems quite similar to the film deposited using glow discharge of He plasma. Figure 4.10 shows the three-dimensional image of that SiO_2-like film made by Ar/N_2 plasma deposited on the silicon wafer that was taken by a laser microscope. A very smooth surface without any spherical particles on it can be observed in that figure. In addition, the thickness of the film appeared to be uniform over the Si wafer surface confirming the homogeneous discharge characteristic of the Ar/N_2 plasma. From these results, it can be concluded that the Ar/N_2 plasma is one of the great potential plasmas and more powerful than the He plasma for depositing SiO_2-like films from organosilicon monomer. More experiments based on Ar/N_2

plasma in place of using He plasma to deposit high quality silica film are still under investigation in our laboratory.

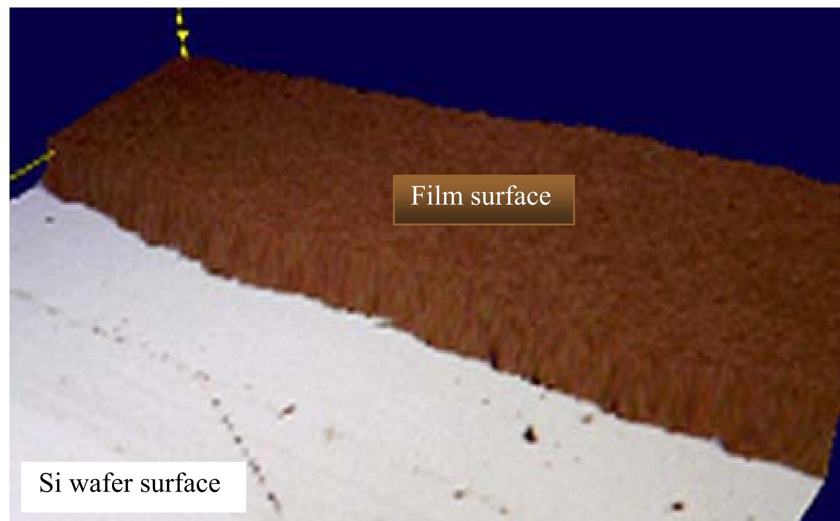

Figure 4.10. Three dimensional image of SiO_2-like film deposited on Si wafer using a glow-like Ar/N_2 plasma with O_2/HMDSO admixture.

Conclusion

A non-equilibrium atmospheric pressure plasma torch that can be sustained either with He or Ar gas has been successfully developed to operate at room temperature. The preparation of SiO_2-like film by means of the plasma torch was investigated using HMDSO as monomer and oxygen as carrier gas. It was found that plasma system based on Ar gas can produce SiO_2-like deposit film much better in chemical composition and growth rate than the film deposited based on He plasma. By using O_2 gas with a flux lower than 100 mL/min through the bubbler, it is possible to obtain the inorganic coating film by atmospheric pressure Ar plasma torch even without substrate heating. In order to improve the quality of the film, homogeneous discharge based on Ar gas is likely to be used to assist the deposition. It has been shown that the addition of small amount of N_2 gas could quench the Ar plasma and yielded a transition of a plasma regime from the filamentary to glow-like discharge when the composition ratio of Ar and N_2 is 30:1. Application of Ar/N_2 glow-like discharge revealed better quality of the deposit film than that produced by using the pure Ar plasma and can become one of the promising alternatives for substituting the expensive He gas in generating plasma at atmospheric pressure.

References

1. Y. Sawada, S. Ogawa and M. Kogoma, *J. Phys D: Appl. Phys.*, **28**, 1661-1669 (1995).

2. R. Foest, F. Adler, F. Sigeneger, M. Schmidt, *Surf. Coat. Technol.*, **163-164**, 323-330 (2003).

3. L.J. Ward, W.C.E. Schofield and J.P.S. Badyal, *Langmuir*, **19**, 2110-2114 (2003).

4. L. O'Neill, L.-A. O'Hare, S. R. Leadley, A. J. Goodwin, *Chem. Vap. Dep.*, **11**, 477-479 (2005).

5. S.E Babayan, J.Y. Jeong, V.J. Tu, J. Park, G.S. Selwyn and R.F. Hicks, *Plasma Sources Sci. Technol.*, **7**, 286-288 (1998).

6. S.E Babayan, J.Y. Jeong, A. Schutze, V.J. Tu, M. Moravej, G.S. Selwyn and R.F. Hicks, *Plasma Sources Sci. Technol.*, **10**, 573-578 (2001).

7. Y. Mori, K. Yoshii, H. Kakiuchi and K. Yasutake, *Rev. Sci. Instrum.*, **71**, 3173 (2000).

8. H. Kakiuchi, Y. Nakahama, H. Ohmi, K. Yasutake, K. Yoshii and Y. Mori, *Thin Solid Films*, **479**, 17-23 (2005).

9. S. Wang, V. Schulz-von der Gathen and H.F. Dobele, *Applied Physics Letters*, **83**, 3272-3274 (2003).

10. Tota P.K., S. Kuroda and H. Kubota, *Plasma Processes and Polymers*, accepted.

11. Sang Hee Lee and Duck Chool Lee, *Thin Solid Films*, **325**, 83-86 (1998).

12. M. Walker, K. -M. Baumgärtner, J. Feichtinger, M. Kaiser, A. Schulz and E. Räuchle, *Vacuum*, **57**, 387-397 (2000).

13. R.W.B. Pearse, A.G. Gaydon, The Identification of Molecular Spectra. Fourth Edition, Chapman and Hall, 1976.

14. A. Kuwabara, S. Kuroda, H. Kubota, *Plasma Processes and Polymers*, **2**, 305-309 (2005).

15. O. Goossens, E. Dekempeneer, D. Vangeneugden, R. Van de Leest and C. Leys, *Surf. Coat. Technol.*, **142-144**, 474-481 (2001).
16. V. Poenariu, M. R. Wertheimer, R. Bartnikas, *Plasma Processes and Polymers*, **3**, 17-29 (2006).
17. A. Qayyum, Shaista Zeb, Shujaat Ali, A. Waheed, M. Zakaullah, *Plasma Chemistry and Plasma Processing*, **25**, 325-351 (2005).
18. A. Belkind, A. Freilich, J. Lopez, Z. Zhao, W. Zhu and K. Becker, *New Journal of Physics*, **7**, 90 (2005).
19. S.E. Alexandrov, N. McSporran, M. L. Hitchman, *Chemical Vapor Deposition*, **11**, 481-490 (2005).
20. A. Bogaerts, R. Gijbels, J. Vlcek, *Spectrochimica Acta Part B*, **53 (11)**, 1517-1526 (1998).
21. R. Lamendola and R. d'Agostino, *Pure & Appl. Chem.*, **70 (6)**, 1203-1208 (1998).
22. F. Palumbo, P. Favia, M. Vulpio, R d'Agostino, *Plasmas and Polymers*, **6**, 163-174 (2001).
23. A. Pfuch, A. Heft, R. Weidl and K. Lang, *Surf. Coat. Technol.*, **201**, 189 (2006).
24. A. Sonnenfeld, T.M. Tun, L. Zajícková, K.V. Kozlov, H.E. Wagner, J.F. Behnke and R. Hippler, *Plasmas and Polymers*, **6**, 237-266 (2001).

CHAPTER VI

SUMMARY

The primary aim of the work described in this thesis focuses to the development of novel non-equilibrium atmospheric pressure plasma and its application to deposit two types of thin solid films; organic films and inorganic films, based on operation by using argon (Ar) as the working gas. In addition to the deposition, attention was directed toward the properties of these films through various characterization methods. The second objective is intended to explore the usage of low pressure plasma to induce graft polymerization of methyl methacrylate onto kenaf fiber having relatively high content of lignin.

The thesis begins in *Chapter I* with a review about plasma, included the history, low temperature plasma parameters, application in polymerization and some problems that still exists during its employment in industry. Based on trying to overcome those problems and learning from many reviewing literatures regarding plasma technology, we have successfully developed a novel plasma jet source that we named it by "Cold Atmosphere Pressure Plasma Torch" or CAPPLAT. It is operated with pulse-modulated high voltage to yield a low temperature discharge at

atmospheric pressure. Configuration of the torch as well as its characterization of the plasma jet is described in *Chapter II*. Electrical diagnostic clarifies that the discharge is a type of homogeneous glow both for helium (He) and Ar plasma as shown by no appearance of spiky lines in their time-dependent current curves. Results from optical emission spectroscopy (OES) showed that reactive species such as $O^{\cdot}$, $OH^{\cdot}$ and various of N_2 system were present when the plasma was generated in open air. Notation should be addressed to the Ar plasma that has the excited species intensity more than 20 orders in magnitude than those in He plasma. The plasma jet length is highly influenced by applied voltage and gas flow rate.

Alongside the torch development, the research has also investigated two types of film deposition using the torch. *Chapter III* described the first deposition, which attends to the synthesizing of thin films bearing organic characteristic of methyl methcrylate (MMA). Combination of Ar gas and MMA bubbler carried by Ar gas as the gas feed to the torch was found to be effective to deposit dense plasma polymerized methyl methacrylate film. The proper Ar carrier gas flow rate should be equal or more than 0.3 L/min to change the filamentary character of the Ar discharge to the glow-like one and gave rise to the film that has chemical structure resembles to the conventional PMMA. Optical emission spectroscopy (OES) of the discharge at the proper condition supports the result that any newly formed excited species were not observed, that suggests the degree of fragmentation of monomer in the plasma phase was quite low.

The second deposition with the intention to deposit thin film bearing inorganic

character from hexametyldisiloxane (HMDSO) can be found in *Chapter IV*. Oxygen gas was used to transport HMDSO from the bubbler. Compared to He plasma, Ar plasma-mediated deposition process has been proven to be more effective to gain a film with higher rate of growth rate. In addition, the flow rate of carrier oxygen gas should be less than 100 mL/min to grant an inorganic character o the film, otherwise, inclusion of organic moieties would be evidenced. Better appearance of film with the same properties can be achieved when a small amount of nitrogen gas (N_2) was admixed to Ar gas as the feed gas of plasma jet. Ar plasma can be quenched by N_2 with the proportional ratio of 30:1 to obtain a glow-like discharge. Combination of Ar and N_2 gas for generating glow-like plasma can provide the films with better quality than the pure Ar plasma.

Finally, in trying to alternate the hydrophilic surface of kenaf fiber to the hydrophobic feature permanently, plasma-induced graft polymerization of MMA onto kenaf was carried out. Description of the study is presented in *Chapter V*. Peroxides that were formed after plasma treatment and exposure to open air were utilized to start thermally grafting of MMA. It was found there was no weight increase of fiber after graft polymerization. The presence of grafting, however, was clarified by characterization of the grafted fiber with FT-IR, XPS and SEM. Kenaf fiber was coated by PMMA in such a way which leads to the unsmoothed coverage of the fiber surface. By allowing the TG/DTG measurement, the thermal stability of grafted sample was higher than the untreated one. Moreover, it was confirmed that the plasma-induced graft polymerization did not affect the bulk properties of the fiber.

List of Achievements

Original Articles

1. Poly(methyl methacrylate) Films Deposited via Non-equilibrium Atmospheric Pressure Plasma Polymerization with Using Argon as the Working Gas, Tota Pirdo Kasih, Shin-ichi Kuroda, Hitoshi Kubota, *Plasma Processes and Polymers*, accepted.
2. Non-equilibrium Atmospheric Pressure Argon Plasma Torch for Deposition of Thin Silicon Oxide Films, Tota Pirdo Kasih, Shin-ichi Kuroda, Hitoshi Kubota, *Chemical Vapor Deposition*, accepted.

List of Presentations

1. *セリウム塩を開始剤に用いた天然ケナフ繊維へのメタクリル酸メチルのグラフト重合*、トタピルドカシ、黒田真一、久保田 仁、第 51 回高分子学会年次大会、横浜、2002 年 5 月 30 日。
2. *Graft Polymerization of Methyl Methacrylate onto Natural Kenaf Fibers Using Ceric Ion as an Initiator*, S. Kuroda, Tota Pirdo K., H. Kubota, The First Chinese-Russian-Korean International Symposium on Chemical Engineering and Material Science, Shenyang, China, 16 September 2002.
3. *Preparation of Kenaf Fiber-Polymer Composite by Graft Polymerization Technique*, S. Kuroda, Tota Pirdo K. H. Kubota, IUPAC-PC 2002, Kyoto, Japan 3 December 2002.
4. *Characterization of Natural Kenaf Fiber-Poly (Methyl Methacrylate) Composite Prepared by Graft Polymerization*, S. Kuroda, Tota Pirdo K. H. Kubota, International Symposium on Kenaf Development and Show, Beijing, China, 12-14 May 2003.

5. *Surface Modification of Kenaf Fiber via Plasma-Induced Graft Polymerization*, Tota Pirdo K, S. Kuroda, H. Kubota, Materiaru Raifu Gakkai, Kiryu, June 2nd – 3rd, 2005.

Book

S. Kuroda, T.P. Kasih and H. Kubota, Graft Polymerization of Methyl Methacrylate onto Natural Kenaf Fibers Using Cerium as an Initiator, in "Advance on Chemical Engineeringand New Material Science", Eds. S.X. Li and L.J. Xiao, Liaoning Science and Technology Publishing House, 94-98 (2002).

ACKNOWLEDGEMENT

There are many people I would like to thank for their encouragement and contribution to the success of this research, either directly or indirectly. I would like to express my sincerest gratitude to Professor Hitoshi Kubota and Associate Professor Shin-ichi Kuroda for giving me the opportunity to start my study in Gunma University. Their valuable guidance and continual supports and lots of encouragements helped me a lot to carry on in the most difficult periods throughout this dissertation research.

Furthermore, the author would like to thank Associate Professor Shoji Takigami at Instrumental Analysis Center (IAC) for the cooperation, technical support and helpful discussions during many research measurements in IAC.

Also I gratefully acknowledge members in Kubota Laboratory, especially to Ms. Fujiko Konoma as a staff and to all students, for their kindly helps and friendly supports that make the lab an enjoyable environment for both working and learning.

Yoneyama Rotary Scholarship that financially supported me over the last two years is also greatly acknowledged.

Finally, my special thanks to my beloved wife Luki Mahanani and my loving son Ramateo Sahala Manurung and my parents with all other family members, especially to Roby`s family for their love and support during the completion of this thesis work. Without them none of this would have been possibly happened.

Kiryu, February 2007

Tota Pirdo Kasih

CHAPTER V

Surface Modification of Kenaf Fiber

Via Plasma-Induced Graft Polymerization

Abstract

Hydrophobic poly(methyl methacrylate) (PMMA) has been grafted onto the surface of kenaf fiber via plasma-induced graft polymerization. The peroxy groups were initially introduced to kenaf fiber through plasma treatment followed by oxidation in air. The peroxides decomposed to initiate the succeeding graft polymerization. The influence of irradiation time and power applied to generate plasma was investigated. The optimal parameter was set up to obtain the maximum amount of peroxides. It was found that the grafting did not yield any increase on fiber weight, therefore the grafted fiber was studied in more detail with examined characterization by FT-IR, XPS, SEM and TG/DTG. Through the XPS study, it was confirmed that the surface chemical composition of grafted kenaf had been changed due to the presence of PMMA. TG/DTG measurement showed that the grafted polymer did not affect the properties of fiber bulk.

5.1 Introduction

Plasma technology which includes plasma treatment and plasma polymerization has been recognized to be an attractive method for surface modification of polymers. Glow discharge plasma consists of radicals, metastable molecules, UV-radiation and charged particles such as electrons and ions. These kinds of active species that are present in a discharge can have reactions through collisions with polymer surface to form variety of new species that are chemically active. These new species can interact with radical species in plasma leading to the formation of new functional groups, and also could become precursors to initiate polymerization when contacted with an incoming monomer. Most of works regarding plasma-induced graft polymerization have so far dealt with surface modification of films or textile fibers,[1-3] and rare research for modification of plant fiber type materials due to its high lignin content. Some reports have been made on the conventional graft polymerization onto plant fibers using chemical solutions,[4,5] however, those processes usually accompanied with damaging bulk fiber. Therefore, in this chapter, low pressure glow discharge is studied to induce graft polymerization of plant fiber.

Many efforts have been reported over the last few decades to the use of plant fiber in preparation of composite material, which is even recently still an active area of research.[6-8] Among the various plant fibers, kenaf *(hibiscus cannabinus L.)* is regarded as one of the most expecting fiber. Kenaf is a fiber crop plant of Malvaceae family and prefers the tropical and subtropical region for the optimal growth. Chemically, kenaf fiber is predominantly composed of cellulose, lignin, hemicellulose and other constituents such as pentosan and ash. Kenaf, a fast growing agro plant that

is harvested for its fiber, has become famous for the potential feature as a composite reinforcement in place of glass fiber in the view of economic and environmental issues, and also has been in competing with flax and hemp fibers on the global market. In addition to increase the value of the product, the usage of kenaf fiber is also considered to the guarantee of the fiber supply continuity.[9]

Instead of many advantages of using kenaf which are mentioned above, kenaf fiber also has drawbacks when it combined with thermoplastics. The main problem of kenaf is its hydrophilic nature due to three hydroxyl groups in the repeating unit of cellulose. In order to modify kenaf fiber physically and chemically to meet the useable requirement, graft polymerization is one of the effective method. However, thinking of the application of kenaf fiber as the reinforcement of composites, kenaf is required to retain its fiber structure after the modification. It has been known that a single fiber of kenaf can have a tensile strength and modulus as high as 480 MPa and 18 GPa respectively.[10,11] Thus, in order to reduce the hydropilicity of the fiber with maintains its bulk high specific properties, special treatment with the plasma-induced graft polymerization as the most likely, must be conducted to the surface of fiber.

The present study has a deal with the plasma-induced graft polymerization of MMA monomer onto kenaf fiber to coat the surface of kenaf fiber with PMMA. The effectiveness of this method to improve the surface is examined by measuring the product with FT-IR, XPS, SEM and TG/DTA. If the hydrophilic of kenaf fiber can be coated by covalently bonded hydrophobic polymer, it will improve the compatibility of kenaf fiber and polymer matrix such as polyethylene, polypropylene or poly(vinyl chloride) in the preparation of composite materials.

5.2 Experimental

Materials

The kenaf fiber from the core part of kenaf plant used was produced in Anhui Province, China and supplied by Uni Corporation, Japan. The average kenaf fiber length was 3 mm and the average diameter about 60-120 μm. Lignin content of the kenaf fiber was 20.6 % through measurement by using Klason method. The fiber was simply washed with boiling water and then dried in a vacuum dryer before plasma-induced graft polymerization experiments. The dried fiber was designated as 'untreated fiber'. Methyl methacrylate monomer was purchased from Wako Pure Chemical Ltd, and was distilled under reduced pressure before used. Tetrahydrofuran (THF) that was utilized as solvent extraction was used as received.

Plasma-induced Graft Polymerization

Plasma-induced graft polymerization of MMA monomer onto kenaf fiber was carried out in two steps of process. First, the activation of kenaf surface by irradiation of air plasma. A commercial bell-jar type plasma reactor (Figure 5.1) was used in this experiment. Kenaf fibers were put into the petri-dish and then were placed on the sample holder at lower electrode. The system was evacuated and the pressure inside of reactor was reduced to 5 Pa, followed by introduction of air into reactor. Flow gas controller was operated to stabilize the pressure at 20 Pa before transmitting 13.56 MHz RF power supply to the electrodes. Plasma was generated at a different electric power and the fiber was exposed to glow discharge for a predetermined period of time.

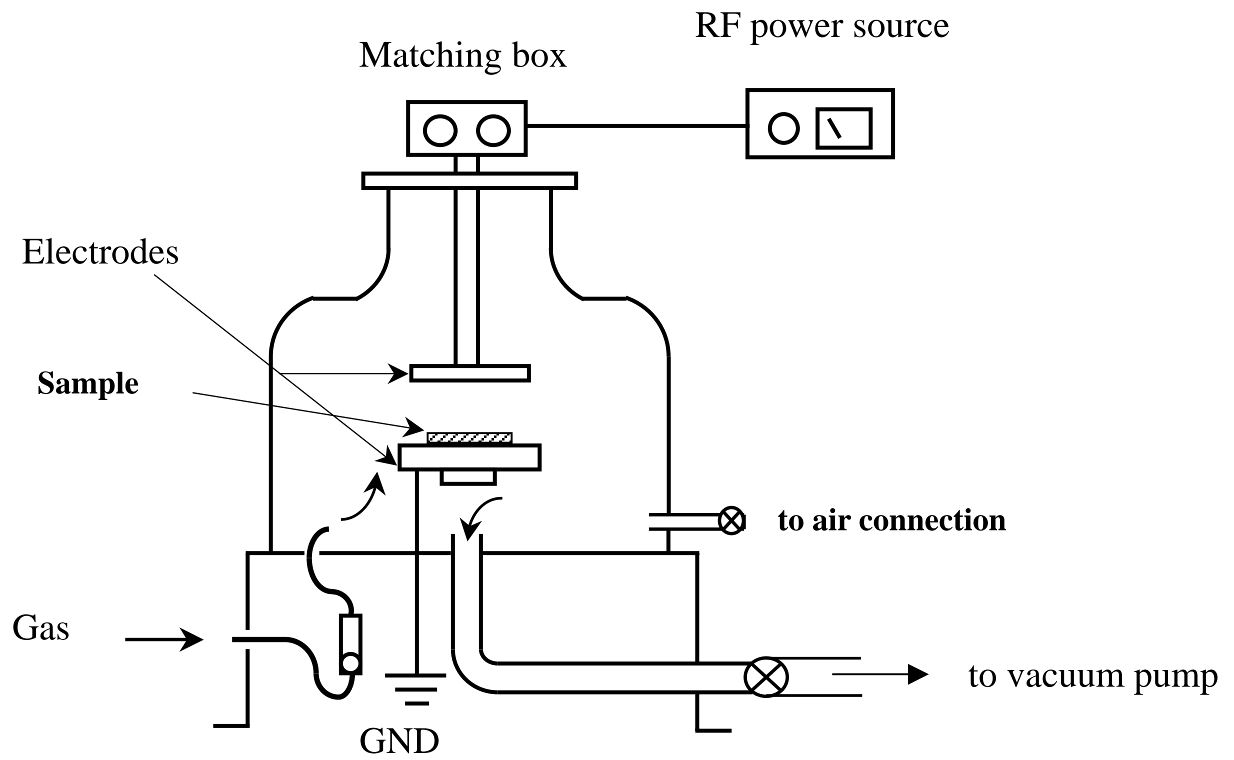

Figure 5.1 Schematic diagram of parallel-plate bell-jar type reactor for plasma treatment of kenaf fiber.

After the plasma treatment, the fibers were contacted with air atmosphere for 5 min to form peroxides on the surface. Secondly, graft polymerization was carried out on the plasma treated kenaf fiber. The fibers containing peroxy groups were placed into the vessel and then immersed in 2 mL MMA monomer aqueous suspension. After degassing thoroughly, the graft polymerization was thermally performed at 60℃ for 5 h. In order to remove any adhered homopolymer, the grafted fibres were extracted with THF over a night.

Formation of Peroxide

The amount of peroxide formed on kenaf surface after plasma treatment and subsequent reaction with air atmosphere was determined according to the iodometric titration with the following procedure:[12]

The plasma treated kenaf were placed in a flask containing solution mixture of 20 mL isopropyl alcohol, 5 mL saturated sodium iodide aqueous solution and 2 mL glacial acetic acid. The mixed solution was refluxed at 85 ℃ for 15 min, and then cooled to the room temperature. The liberated iodine was then titrated with 0.01 N standard sodium thiosulfate solution.

Measurements for Characterization

The infrared (IR) spectra of MMA-grafted kenaf fibers were recorded on a Jasco FT-IR-8000 spectrophotometer, with using their KBr disks.

Scanning electron microscopy (SEM) was used to examine the surface

morphology of untreated and grafted fibers. SEM of those fiber samples was observed using a Jasco JSM-5300 device.

Thermogravimetric analysis was conducted to measure the thermal degradation of the original and grafted kenaf fiber with using a SEIKO TG/DTA instrument. The initial sample weight was in the range 4 - 5 mg. TG curves were obtained in the temperature range from room temperature to 500 ℃ under a nitrogen atmosphere with a heating rate of 20 ℃/min.

XPS analysis was performed using a Perkin Elmer ESCA 5600 instrument. Unmonochromated Mg Kα radiation (1253.6 eV) was used from the dual anode X-ray source for photoelectron excitation. The X-ray source was operated at 400W and 15 kV. The angle between the X-ray source and analyzer was fixed at 45° . The wide scan (1.6 eV resolution) and high resolution scan (0.25 eV resolution) were carried out and the C1s spectra were deconvoluted for the analysis using a curve fitting program of MultiPak Software V.6.1A.

5.3. Results and Discussion

Formation of Peroxide

It is generally known that oxygen containing functional groups can be introduced onto the surface of plasma-treated polymers in the form of carboxyl, ketone, hydroxyl and peroxide.[10] Among those groups, the peroxide is the most possible active species that can initiate graft polymerization in the presence of monomer. Table 5.1 summarizes the formation of peroxides on kenaf fiber surface

Table 5.1. Effect of Irradiation Time and Power Applied of Air Plasma on the Formation of Peroxides on Kenaf Fibers.

Sample	Irradiation time (s)	RF power (W)	Amount of peroxide (meq/100 g sample)
Untreated fiber	---	---	0
Treated fiber	30	5	0.49
	60	5	0.69
	120	5	1.09
	180	5	1.49
	300	5	1.39
	180	2.5	0.49
	180	5	1.49
	180	10	1.29
	180	15	0.49
	180	25	0.20

after the irradiation of air plasma and 5 min exposure to air atmosphere as a function of plasma irradiation time and plasma power. The maximum amount of peroxide has been obtained when the fiber was irradiated by plasma for 180 s at 5 W of plasma power that gave a concentration of peroxide of 1.49 meq/100 g sample. It can also be observed that increasing the plasma power as well as elongating the plasma irradiation time did not result in more peroxides. The parameters set of 180 s and 5 W were therefore used for subsequent thermal graft polymerization of MMA onto kenaf fiber.

Plasma-induced Graft Polymerized Sample

The thermal graft polymerization of MMA on plasma-treated kenaf fiber was carried out at 60℃ for 5 h. The grafting has been conducted for the different plasma treatment time, however, the similar results have been obtained in the view that there was no weight increase in grafted kenaf fiber after extraction with THF. The presence of grafting therefore was examined by using the following analyses during the characterization of grafted fiber. The samples for characterizations were taken from parameter plasma treatment that produces the maximum amount of peroxides for the effectiveness of the grafting.

FT-IR Spectra

The FT-IR spectra of untreated and grafted kenaf fiber are shown in Figure 5.2. Figure 5.2.a. shows a typical kenaf spectrum, which carries a broad absorption band of hydroxyl group around 3400 cm^{-1}, C – H stretching band around 2910 cm^{-1} and an

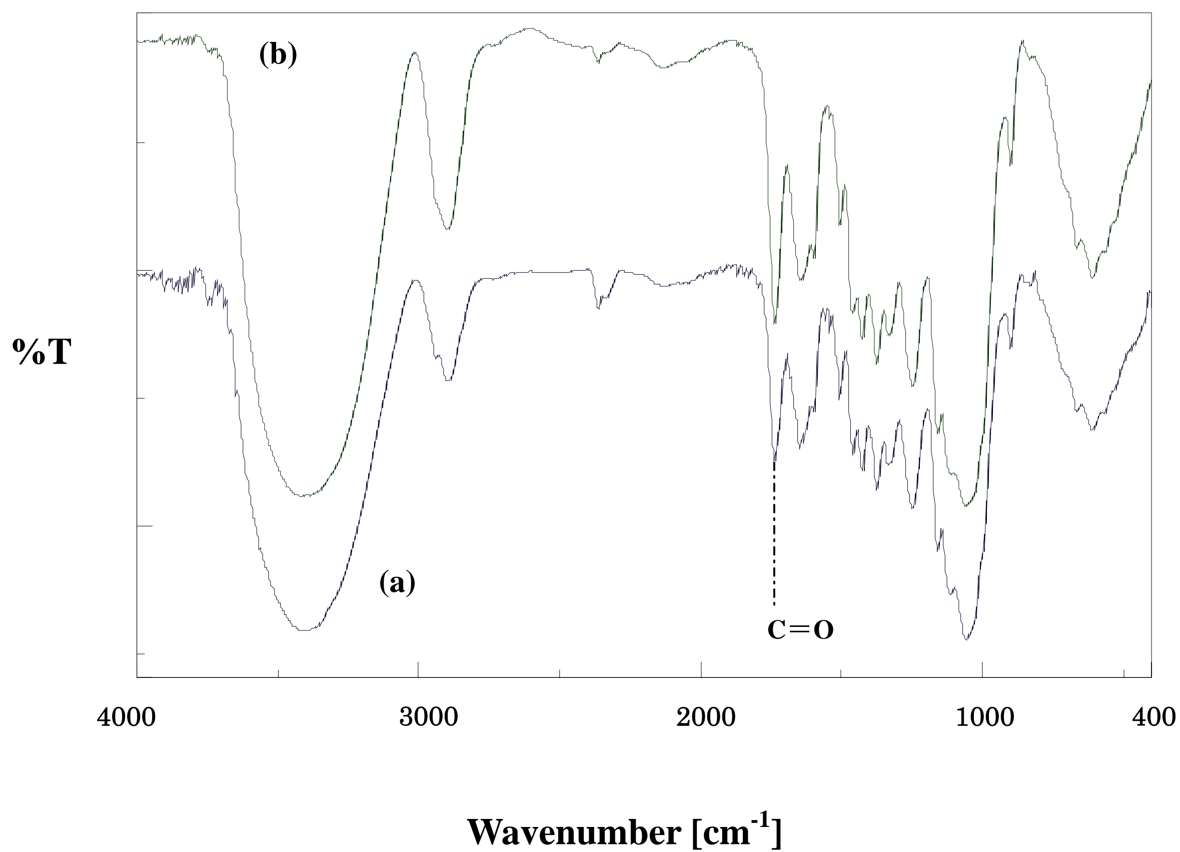

Figure 5.2. FT-IR spectra of untreated kenaf fiber (a) and grafted kenaf fiber (b).

absorption band around 1100 cm^{-1} associated to the ether linkage in the pyranoside ring. It is observed that the FT-IR spectrum characteristic of grafted fiber (Figure 5.2.b.) is similar to that of the untreated one, except an increase in intensity of ester groups near 1738 cm^{-1}. This additional band indicates the presence of PMMA in the grafted fiber. Kenaf fiber has shown the peak near 1738 cm^{-1}, which may arise from the unconjugated carbonyl group in lignin. From the preliminary experiment, it has been clarified that the lignin content of the used kenaf fiber was 20.6 %, which was relatively higher than wood or any textile materials. Therefore, grafting of PMMA onto kenaf was only identified by the increase of this peak intensity.

X-ray Photoelectron Spectroscopy (XPS) Study

XPS is a surface sensitive analysis used to determine the surface atomic composition and to know the chemical state of the atoms. In this study, XPS measurements were performed to investigate the changes in chemical composition and to identify the chemical bonding existing on the surface of untreated and grafted kenaf fibers. Figure 5.3 shows the high resolution scans of the C1s core spectrum with their deconvolution peaks for the untreated kenaf fiber (5.3.a) and grafted kenaf (5.3.b). It can be seen that the C1s core spectrum of untreated kenaf fiber consists of four different peaks at 284.5 eV for C—H/C—C, at 286.5 eV for C—O, at 288.1 eV for C=O/O—C—O and at 290 eV for O—C=O. Characteristics of kenaf fiber surface are mostly indicated by C—O and C=O/O—C—O, among which C—O and O—C—O are the characteristic of for the pure cellulose.[18,19] However, rather high

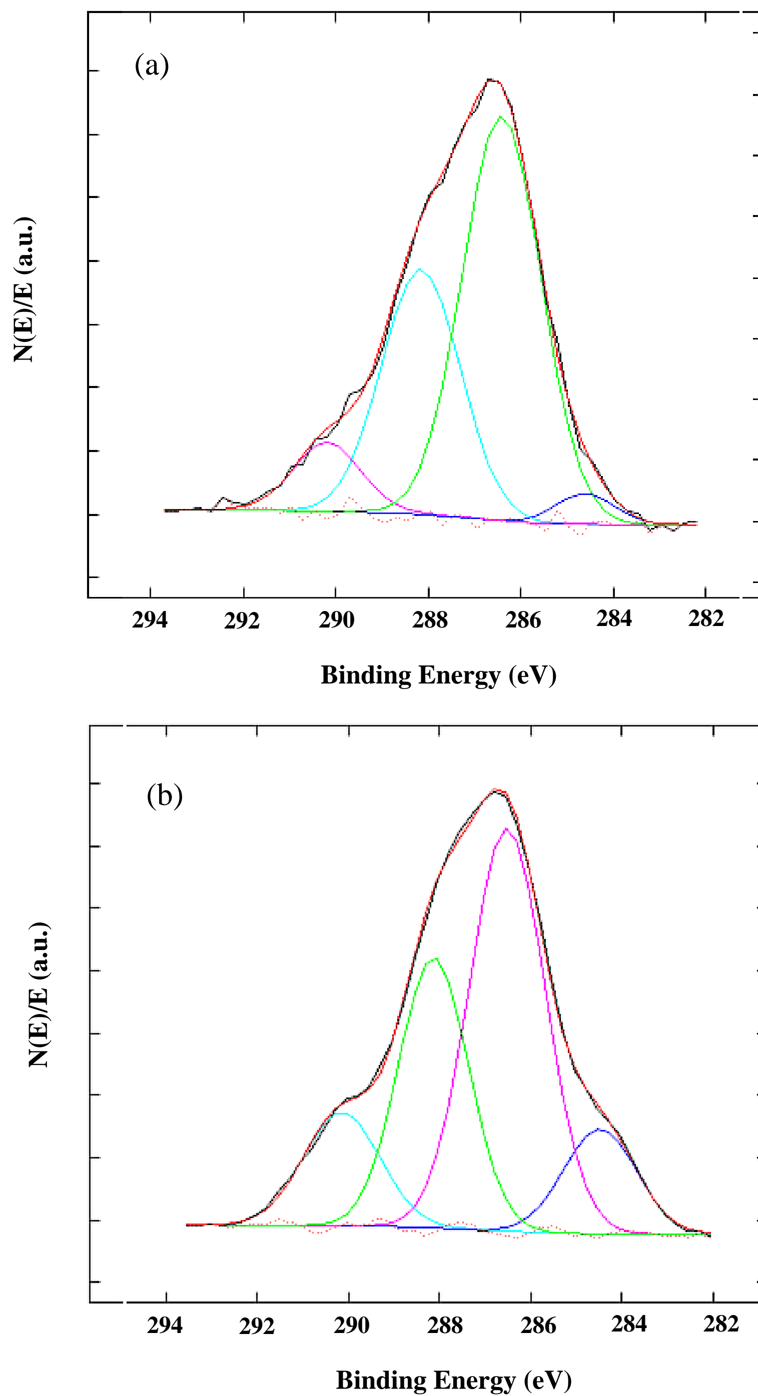

Figure 5.3 High resolution of C1s core spectra of untreated kenaf fiber (a) and plasma grafted kenaf fiber (b).

content of 288.1 eV peak and the lower percentage C－C and O－C＝O components suggest that some hydrocarbon-rich compounds like lignin and some extractive compounds such as fat or wax are mixed well with cellulose and are present on the fiber surface. This is plausible since the raw kenaf was only extracted with hot water, which could not remove some compounds mentioned above from kenaf fiber. Plasma graft polymerization of PMMA onto kenaf fiber clearly makes differences on the fiber surface compared to the untreated one, where an increase in peak intensity of C－C and O－C＝O bonds can be observed. The relative chemical bonds concentrations from C1s core spectra deconvolution of untreated and grafted fibers are summarized in Table 5.2. Compared to the untreated fiber, an increase in C－C concentration up to 11.6% and a significant increase in O－C＝O concentration to 13.2% due to the incorporation of methylene, methyl and ester groups of PMMA are apparent for the grafted fiber. Accompanied to those increase are the decreases in C－O and C＝O/O－C－O concentrations. These facts clearly indicate the grafting of PMMA on kenaf fiber. However, the existence of C＝O/O－C－O component of the grafted fiber tells that the untreated kenaf fiber is still detected by the XPS because it is absent in PMMA. If the grafted PMMA covers thoroughly the kenaf fiber, the chemical composition of grafted fiber should be similar to that of PMMA surface. The obtained result, however, does not agree with it, suggesting that the plasma-induced grafting of PMMA occurs only to some extent to cover partial surface of kenaf fiber. The surface area with grafted PMMA can be estimated as 15 % based on the concentrations of

Table 5.2. Relative Chemical Components Concentration from Deconvolution of C1s Core Spectra of Untreated Kenaf Fiber and Grafted Kenaf Fiber.

Sample	C−H / C−C	C−O	C=O / O−C−O	O−C=O
Untreated kenaf	3.1	54.9	33.4	8.6
Grafted kenaf	11.6	46.6	28.7	13.2

C—H/C—C and C=O/O—C—O components. On the other hands, the calculated areas based on the C—O and O—C=O concentrations were estimated as 25 % and 40 % respectively, which might be caused by the enrichment of these components on kenaf fiber through plasma treatment. The XPS study mentioned above leads to a conclusion that PMMA had been graft polymerized onto kenaf fiber surface, but the coverage did not occur to all surface of fiber. The SEM measurements were thus conducted to complement the XPS study.

SEM Micrograph

Surface morphology of untreated and grafted fibers is shown in SEM images depicted in Figure 5.4. It can be observed from Figure 5.4.a that the untreated kenaf fiber has a rather smooth surface originally. Several fibrils are bound together by middle lamella consisting mainly of lignin. The middle lamella was not removed because the extraction of fiber had been conducted only with hot water. Typical natural fiber extraction with alkali solution can remove such contaminants, however, sometimes causing damages to the fiber, which thus decreases the mechanical properties. On the other hand, the grafted kenaf surface seems to be masked with polymer (Figure 5.4.b). The PMMA masks can be seen covering the fiber in such a way which lead to the unsmoothed coverage of the fiber surface. No such damages were found on the individual fibers. This result has an agreement with preceding results of XPS measurements. The incomplete coverage of fiber surface could be attributed to the inhomogeneous interaction between fiber surface and plasma. It is considered that the

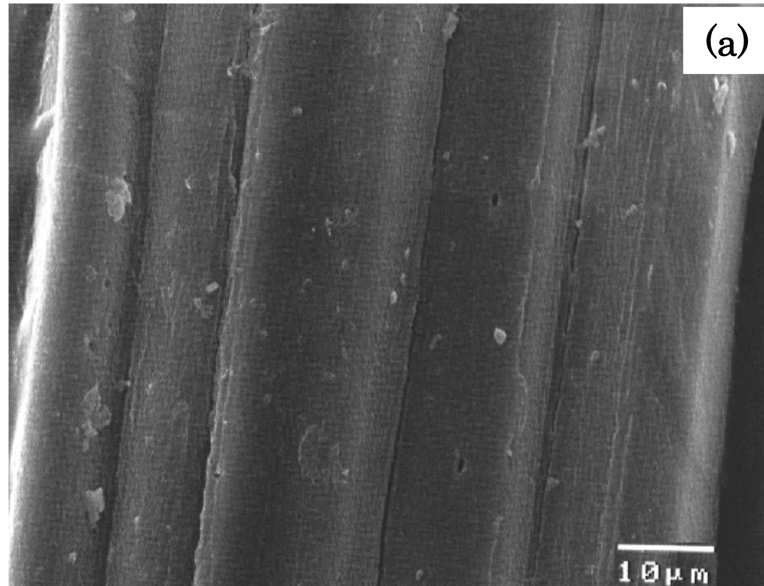

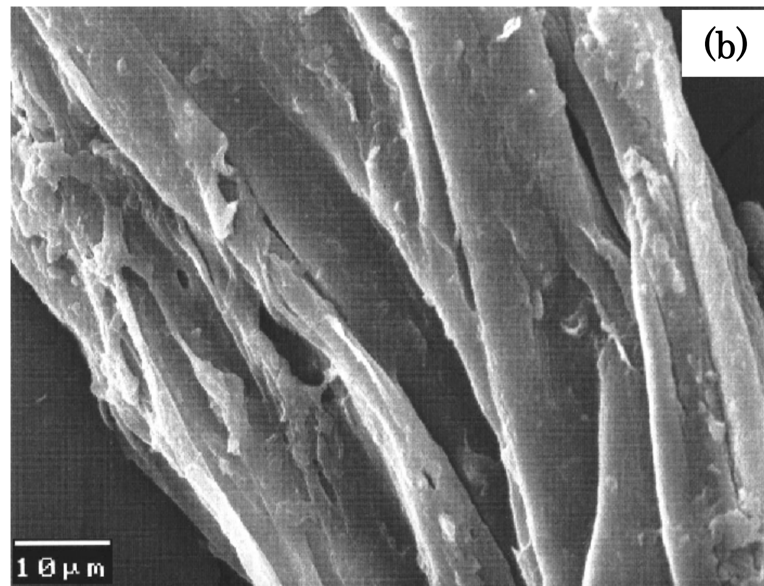

Figure 5.4 SEM images of untreated kenaf fiber (a) and grafted kenaf fiber (b).

activation of fiber surface occurred only on the surface facing in a certain direction to the glow discharge. In addition, the surface activation reaction was thought not to occur on the underlying region of fiber surface. Another plausible reason is caused by the roughness and unevenness surface of kenaf (Figure 5.4.a) that cause it variably susceptible to plasma treatment.[20] Nevertheless, this plasma-induced graft polymerization has been proved to modify the kenaf fiber surface without altering the bulk properties.

Thermal Behavior (TG/DTG)

Both of untreated and MMA-grafted kenaf fibers were subjected to thermogravimetry (TG/DTG) analysis, and the results are utilized to elucidate the typical changes of their thermal behavior. Figure 5.5 represents the TG and DTG curves of untreated and grafted kenaf fibers. It can be seen that the overall weight loss of untreated fiber during thermal degradation could be divided into three different steps. In the first step, weight loss occurs below 100℃ with about 7 % of initial weight, which is attributed to the evaporation of absorbed water from the fibers. In the second step, the fiber loses its 20 % weight. This is the initial stage of thermal degradation that occurs around 300℃, represented by a shoulder in DTG curve. The last step relating to the major thermal degradation shows a maximum weight loss rate at 374℃. Concerning with the grafted fiber, it could be observed that the general features of the curves are similar to those of the untreated one except the decelerated weight loss below 100℃ and the total shift to the right. The former should be the

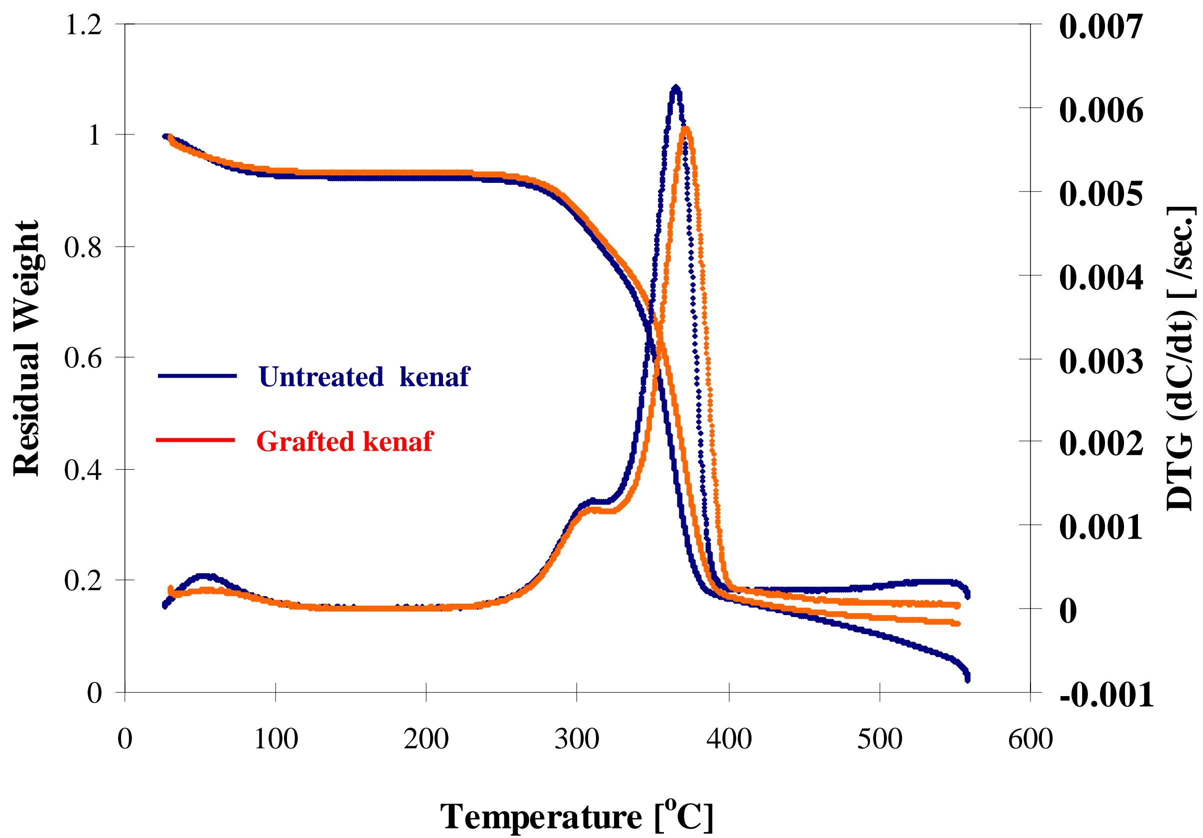

Figure 5.5. TG and DTG curves of untreated kenaf fiber (a) and grafted kenaf fiber (b).

effect of PMMA layer with low vapor permeability. On the other hand, the latter shows that the thermal stability of grafted kenaf fiber is higher than untreated kenaf fiber. This founding is interesting since the PMMA itself decomposed completely at 375℃, thus the grafting of PMMA onto kenaf should lower its thermal stability. This phenomenon can be explained that graft polymerization forms a sort of cross linking with kenaf molecule. The breakage of various linkages by plasma treatment could be compensated by this new type of crosslink formed simultaneously with grafting, leading to the enhancement of thermal stability due to lower mobility molecules. This is also supported by the relatively large amount of the char residue for grafted fiber compared to the untreated one.

CONCLUSIONS

In this work, plasma-induced graft polymerization of MMA monomer onto kenaf fiber using air plasma was studied. Peroxy groups were formed and became the active species to proceed the grafting. The amount of peroxides generated by plasma treatment and successive reaction with air apparently depended on the plasma irradiation time and power applied. It was found that that there was no weight increase in grafted kenaf fiber after extraction with solvent. Some measurements such as FTIR, XPS, SEM and TG/DTG were used to investigate the changes of surface chemical composition after grafting. It was clarified that the graft polymerization of MMA onto kenaf fiber had been occurred on the partial surface of kenaf fiber, and improve the thermal stability of the fiber.

References

1. B. Gupta, J. G. Hilborn, I. Bisson, P. Frey, *Journal of Applied Polymer Science*, **81**, 2993-3001 (2001).
2. Nguyen K. C, N. Saeki, S. Kataoka and S. Yoshikawa, *Hyomen Kagaku*, **23**, 202-208 (2002).
3. Hartwig Hocker, *Pure Appl. Chem.*, **74**, 423-427 (2002).
4. I. C. Eromosele, A. Agbo, *Journal of Applied Polymer Science*, **73**, 1751 (1999).
5. Ighodalo C. Eromosele, Solomon S. Bayero, *Journal of Applied Polymer Science*, **73**, 1751 (1999).
6. H.L. Chen and R.S. Porter, *J. of Appl. Polym. Sci.,* **54**, 1781-1783 (1994).
7. A.R. Sanadi, D.F. Caulfield, R.E. Jacobson and R.M. Rowell, *Ind. Eng. Chem. Res.,* **34**, 1889-1896 (1995).
8. D. Feng, D.F. Caulfield and A.R. Sanadi, *Polymer Composites*, **22**, 506 (2001).
9. R.M. Rowell, Proceeding of the 18th International Symposium on Material Science: Polymeric Composites – Expanding the Limit, Roskilde, Denmark, 127 (1997).
10. J. Xu, R. Widyorini, S. Kawai, *Journal of Wood Science*, **51**(4), 415-420 (2005).
11. Kawai S., Sasaki H., Yamauchi H., 1st Wood Mechanics Conference, Lausanne, 503–514 (2001).
12. Ginting S. I., PhD Thesis Department of Chemistry, Gunma University, 2003.
13. M. Suzuki, A. Kishida, H. Iwata and T. Ikada, *Macromolecules*, **19**, 1804 (1986).
14. N. Inagaki, S. Tasaka, Y. Goto, *Journal of Applied Polymer Science*, **66**, 77 (1997).
15. L.M. Matuana, J.J. Balatinecz, R.N.S. Sodhi, C.B. Park, *Wood Science and Technology*, **35**, 191-201 (2001).
16. G. Beamson and D. Briggs, High resolution XPS of Organic Polymers: the Scienta ESCA300 database, Wiley, New York, 1992.
17. N. Abidi, Eric Hequet, *Journal of Applied Polymer Science*, **93**, 145-154 (2004).
18. David N.-S. Hon, *Journal of Applied Polymer Science*, **29** (9), 2777-2784 (1984).
19. Pawel Zadorecki, Tore Rönnhult, *Journal of Polymer Science Part A: Polymer Chemistry*, **24** (4), 737-745 (1986).

20. Johan Felix, Paul Gatenholm, H. P. Schreiber, *Journal of Applied Polymer Science*, **51**, 285-295 (1994).
21. Y.C. Ma, S. Manolache, M. Sarmadi, F. S. Denes, *Starch – Stärke*, **56**, 47 (2004).
22. D. P. Kamdem, B. Riedl, A. Adnot, S. Kaliaguine, *Journal of Applied Polymer Science*, **43** (10), 1901-1912 (1991).
23. Terrence G. Vargo, Joseph A. Gardella Jr., Lawrence Salvati Jr., *Journal of Polymer Science Part A: Polymer Chemistry*, **27** (4), 1267-1286 (1989).
24. Chee-Chan Wang, Ging-Ho Hsiue, *Journal of Polymer Science Part A: Polymer Chemistry*, **31** (5), 1307-1314 (1993).
25. Ging-Ho Hsiue, Chee-Chan Wang, *Journal of Polymer Science Part A: Polymer Chemistry*, **31** (13), 3327-3337 (1993).
26. H.P., L. Viikari, *Biotechnology and Bioengineering*, **86** (5), 550-557 (2004).
27. M. G. McCord, Y. J. Hwang, Y. Qiu, L. K. Hughes, M. A. Bourham, *Journal of Applied Polymer Science*, **88** (8), 2038-2047 (2003).
28. N. Inagaki, S. Tasaka, T. Inoue, *J. of Applied Polymer Science*, **69**, 1179 (1998).
29. G. Canché-Escamilla, G. Rodríguez-Trujillo, P. J. Herrera-Franco, E. Mendizábal, J. E. Puig, *J. of Appl. Polym. Sci.*, **66** (2), 339-346 (1997).